U.S. Fish & Wildlife Service

Arcata Fisheries Technical Report TR 2018-33

Estimating Freshwater Productivity, Overwinter Survival, and Migration Patterns of Klamath River Coho Salmon

Christopher V. Manhard, Nicholas A. Som, Russell W. Perry,
Jimmy R. Faukner and Toz Soto

U.S. Fish and Wildlife Service
Arcata Fish and Wildlife Office
1655 Heindon Road
Arcata, CA 95521
(707) 822-7201

February 2018

Funding for this study was provided by a variety of sources, including the Klamath River Fish Habitat Assessment Program administered by the Arcata Fish and Wildlife Office and the Bureau of Reclamation Klamath Falls Area Office.

Disclaimer: The mention of trade names or commercial products in this report does not constitute endorsement or recommendation for use by the Federal Government. The findings and conclusions in this report are those of the authors and do not necessarily represent the views of the U.S. Fish and Wildlife Service.

The Arcata Fish and Wildlife Office Fisheries Program reports its study findings through two publication series. The **Arcata Fisheries Data Series** was established to provide timely dissemination of data to local managers and for inclusion in agency databases. **Arcata Fisheries Technical Reports** publish scientific findings from single and multi-year studies that have undergone more extensive peer review and statistical testing. Additionally, some study results are published in a variety of professional fisheries aquatic habitat conservation journals.

To ensure consistency with Service policy relating to its online peer-reviewed journals, Arcata Fisheries Data Series and Technical Reports are distributed electronically and made available in the public domain. Paper copies are no longer circulated.

key words: Population Dynamics, Productivity, Survival, Movement, Coho Salmon

The correct citation for this report is:

Manhard, C. V., N. A. Som, R. W. Perry, J. R. Faukner, and T. Soto. 2018. Estimating freshwater productivity, overwinter survival, and migration patterns of Klamath River Coho Salmon. U.S. Fish and Wildlife Service. Arcata Fish and Wildlife Office, Arcata Fisheries Technical Report Number TR 2018-33, Arcata, California.

Table of Contents

List of Tables

page

page

page

page

List of Figures

page

Estimating Freshwater Productivity, Overwinter Survival, and Migration Patterns of Klamath River Coho Salmon

Christopher V. Manhard[1,2], Nicholas A. Som[1,*], Russell W. Perry[3], Jimmy R. Faukner[4], and Toz Soto[5]

[1]*U.S. Fish and Wildlife Service, Arcata Fish and Wildlife Office*
1655 Heindon Road, Arcata, California

[2]*U.S. Geological Survey, California Cooperative Fish and Wildlife Research Unit*
1 Harpst Street, Arcata, California

[3]*U.S. Geological Survey, Western Fisheries Center, Columbia River Research Laboratory*
5501A Cook-Underwood Road, Cook, Washington

[4]*Yurok Tribal Fisheries, Lower Klamath Division*
190 Klamath Boulevard, Klamath, California

[5]*Karuk Department of Natural Resources*
Orleans, California

[*]*Corresponding author*
nicholas_som@fws.gov

Abstract.— An area of great importance to resource management and conservation biology in the Klamath Basin is balancing water usage against the life history requirements of threatened Coho Salmon. One tool for addressing this topic is a freshwater dynamics model to forecast Coho Salmon productivity based on environmental inputs. Constructing such a forecasting tool requires local data to quantify the unique life history processes of Coho Salmon inhabiting this region. Here, we describe analytical methods for estimating a series of sub-models, each capturing a different life history process, which will eventually be synchronized as part of a freshwater dynamics model for Klamath River Coho Salmon. Specifically, we draw upon extensive population monitoring data collected in the basin to estimate models of freshwater productivity, overwinter survival, and migration patterns. Our models of freshwater productivity indicated that high summer temperatures and high winter flows can both adversely affect smolt production and that such relationships

are more likely in tributaries with naturally regulated flows due to substantial intra-annual environmental variation. Our models of overwinter survival demonstrated extensive variability in survival among years, but not among rearing locations, and demonstrated that a substantial proportion (~ 20%) of age-0+ fish emigrate from some rearing sites in the winter. Our models of migration patterns indicated that many age-0+ fish redistribute in the basin during the summer and winter. Further, we observed that these redistributions can entail long migrations in the mainstem where environmental stressors likely play a role in cueing refuge entry. Finally, our models of migration patterns indicated that changes in discharge are important in cueing the seaward migration of smolts, but that the nature of this behavioral response can differ dramatically between tributaries with naturally and artificially regulated flows. Collectively, these analyses demonstrate that environmental variation interacts with most phases of the freshwater life history of Klamath River Coho Salmon and that anthropogenic environmental variation can have a particularly large bearing on productivity.

Introduction

Coho Salmon (*Oncorhynchus kisutch*) that inhabit the Klamath Basin are part of the southern Oregon and northern California Evolutionarily Significant Unit (ESU), which has been recognized as threatened under the Endangered Species Act. Agricultural and industrial practices in the Klamath Basin, such as mining, logging, ranching, and hydropower generation, have impacted the ability of the basin to support production of Coho Salmon. The declining productivity of the basin is evident in the historically low abundances of spawning Coho Salmon that have been observed in recent years in the Scott and Shasta Rivers, two of the primary Coho Salmon production tributaries in the basin (Knechtle and Chesney 2015; Chesney and Knechtle 2015). Of particular concern to Coho Salmon conservation is the impact of water management in the basin on productivity. Five hydropower dams, constructed in the upper reaches of the Klamath River during the first half of the 20th century, impact the hydrology of the mainstem, contributing to reduced summer discharge, elevated water temperature, and impaired water quality downstream of the dams (Stocking and Bartholomew 2007). Water releases from Iron Gate Dam, the lowest of these dams and the upper limit of anadromy in the basin, likely have a particularly significant bearing on the quality of the environment that Coho Salmon experience during their occupancy of the mainstem. Further, the Scott and Shasta Rivers are subjected to major water storage or agricultural diversions beginning in late spring and extending through summer, which dramatically alter the hydrology of these Coho Salmon production zones during critical life history stages.

Given that alterations to the hydrology of the Klamath River and several of its most important production tributaries may critically impact Coho Salmon at several different freshwater life stages, it is necessary to consider the potential outcomes of water management decisions. A potentially effective tool for predicting such outcomes is a freshwater dynamics model that uses environmental variation to forecast the size and abundance of smolts emigrating from the Klamath River, which represent the freshwater output of the basin. Forecasting these attributes requires full consideration of the suite of

life history processes that drive them, including the relationship between spawner abundance and smolt yield, the timing of migratory events, overwinter survival rates, and growth patterns. These processes may be captured through the development of a synchronized series of sub-models, each quantifying the relationship between environmental variation and a life history process. A benefit of this method of model synthesis is that sub-models can be updated as new data and analyses arise. The protracted freshwater residency of Klamath Basin Coho Salmon and the challenges posed by seasonal deterioration of water conditions in many parts of the basin have given rise to a life history that can entail multiple migrations among habitats during the freshwater rearing period. Because of these unique features of their life history, constructing a reliable forecasting tool for Klamath Basin Coho Salmon requires that sub-models are, to the greatest extent possible, estimated from local data.

During recent years there have been substantial efforts to monitor movement and survival of Coho Salmon in the Klamath Basin. These efforts have been conducted by state, federal, tribal, and academic entities and have drawn upon diverse sampling methods. The California Department of Fish and Wildlife (CDFW) has operated video counting weirs and rotary screw traps on several of the major production tributaries which provide a basis for evaluating spawner-recruit relationships and for evaluating the timing of the migrations of juveniles and adults. The Yurok Tribal Fisheries Program (YTFP) and the Karuk Department of Natural Resources (KDNR) have conducted extensive monitoring of fish implanted with passive integrated transponders (PIT) tags by using a combination of traps and stationary interrogation arrays, and the data collected from these studies provide a basis for evaluating migration patterns and overwinter survival rates. We sought to draw upon these rich sources of information in estimating sub-models that captured links between environmental variation and life history processes. The sub-models represent a major contribution to the development of a freshwater dynamics model for Klamath Basin Coho Salmon. This report details our use of the aforementioned sources of data in quantifying (1) relationships between spawner abundances and abundances of emigrant parr and smolts in the Scott and Shasta Rivers; (2) variation in overwinter survival and winter emigration probability among tributaries and years; (3) environmental drivers of the timing of the adult, parr, and smolt migrations in the Scott and Shasta Rivers; (4) environmental drivers of the timing of the summer redistribution, winter redistribution, and smolt migration for tributaries with natural flow regimes; and (5) variation in mainstem migration rates of parr during summer and winter redistribution events. This report is not intended to represent a cohesive freshwater dynamics modelling framework for Klamath Basin Coho Salmon, which will follow in companion documents to this report. Instead, this report serves as documentation of analytic methods, and analysis results, for an extensive collection of statistical analyses that will be used to inform component sub-models of a larger freshwater Coho Salmon population dynamics model for the Klamath Basin.

Methods

Data sources: weirs and rotary screw traps

Video counting weirs ·

Fish counting facilities are operated by CDFW on the Scott River, Shasta River, and Bogus Creek to monitor the Chinook and Coho salmon spawning migrations (Chesney and Knechtle 2016; Knechtle and Chesney 2016). The Scott River, Shasta River, and Bogus Creek fish counting facilities are located 29.3, 0.2, and 0.5 kilometers upstream of their respective stream mouths (Figure 1). Each facility uses a temporary, Alaskan-style weir to direct fish into a flume where they are monitored by a video camera. Facilities are typically operated 24 hours a day, seven days a week from October through December and generally capture most of the Coho Salmon spawning migration. However, high discharge levels necessitate early removal of the weir in some years, potentially resulting in underestimates of spawner abundance. Annual abundance estimates of adult Coho Salmon were derived from direct counts of fish observed at the video counting facility. Further, spawning ground surveys were conducted on the Scott River to account for fish spawning in the 29.3 kilometers below the weir. Redd counts made downstream of the weir were multiplied by two and then added to the count from the video facility to yield an annual abundance estimate[1]. We estimated the freshwater productivity models with annual estimates of adult abundance in the Scott and Shasta Rivers (Tables 1 and 2). We estimated the adult migration timing models with weekly count data from the Scott River, Shasta River, and Bogus Creek (Table 3) which we extracted from technical reports with the package digitize (Poisot 2011) in R (R Core Team 2015).

Rotary screw traps ·

Surveys of age-0+ (parr) and age-1+ (smolts) Coho Salmon emigrating from the Scott River have been conducted by CDFW since 2001 (Chesney and Knechtle 2016; Knechtle and Chesney 2016). Annual juvenile abundances (Tables 1 and 2) were estimated from raw counts of fish captured in rotary screw traps located on the Scott and Shasta Rivers, 7.6 km and 0.1 km upstream of their respective confluences with the Klamath River (Figure 1). In most years, trap efficiencies were estimated from a mark-recapture framework and then used to estimate abundances from raw counts (Carlson et al. 1998). In years where inadequate numbers of Coho Salmon were captured or marked to estimate independent trap efficiencies, correlations between capture efficiencies of juvenile Coho Salmon and juvenile steelhead trout from prior years were instead used to estimate abundance. We estimated the freshwater productivity models with annual estimates of parr and smolt abundance in the Scott and Shasta Rivers (Tables 1 and 2), and we estimated the parr and smolt emigration timing models with weekly abundance estimates for each life stage (Tables 4 and 5).

[1] This method assumes a 1:1 sex ratio, one female per redd, and 100% observer efficiency. It was not possible to confirm that these assumptions were met, based on information presented the CDFW technical reports.

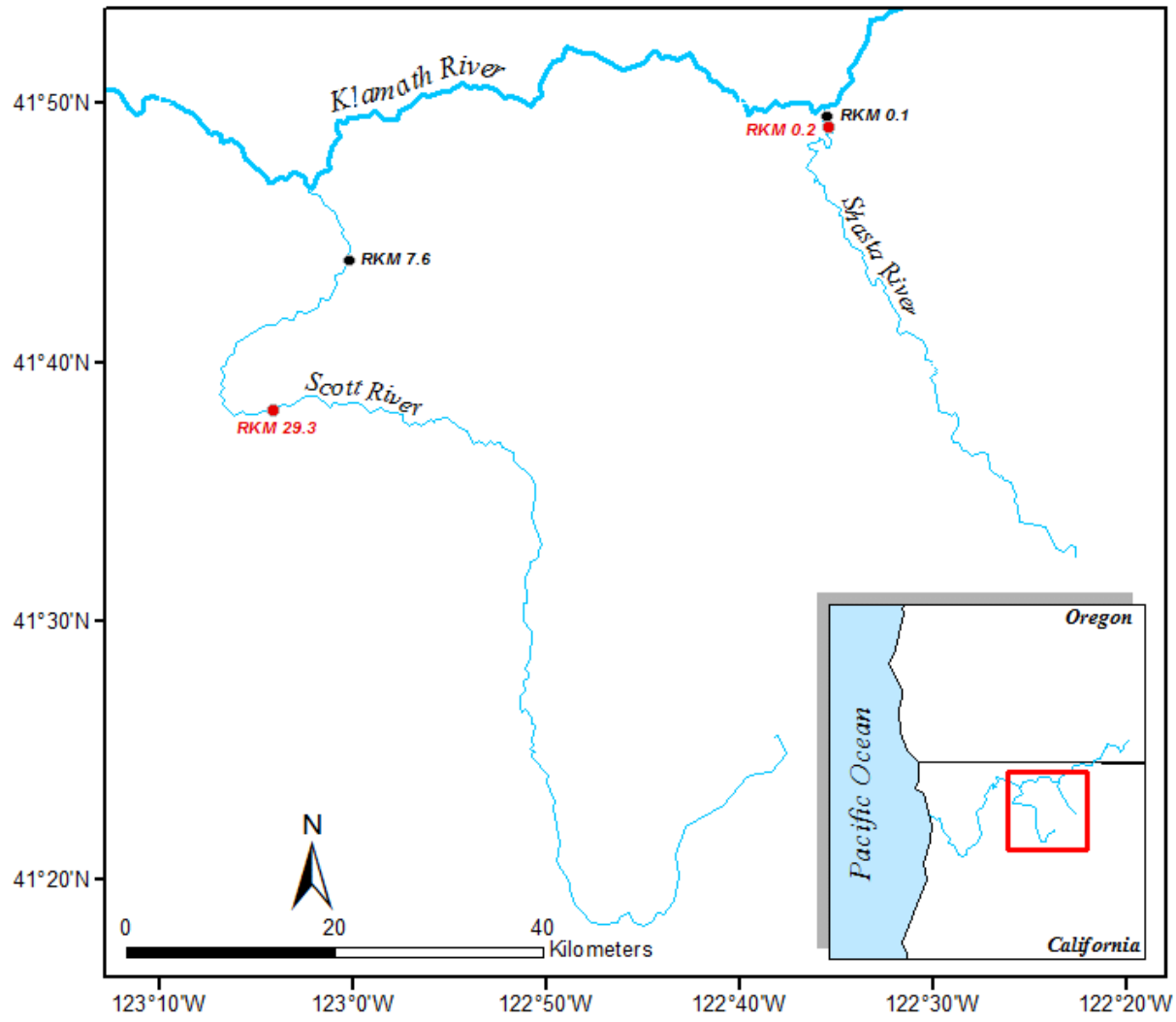

Figure 1. Locations of rotary screw traps (red points) and video counting weirs (black points) in the Scott River, Shasta River, and Bogus Creek in California, USA.

Table 1. Annual abundance estimates of Scott River spawners ($\hat{S}_t$), outmigrating parr ($\hat{J}_{t+1}$), and outmigrating smolts ($\hat{J}_{t+2}$) used to estimate freshwater productivity models. The dates on which the weir was removed and the methods used to estimate juvenile abundance are each listed.

Adult year	Weir removed	$\hat{S}_t$	Parr year	Estimation method	$\hat{J}_{t+1}$	Smolt year	Estimation method	$\hat{J}_{t+2}$
2007	Dec 31, 2007	1,622	2008	mark-recapture	6,645	2009	mark-recapture	62,207
2008	Dec 27, 2008	63	2009	mark-recapture	3,899	2010	steelhead correlation	2,174
2009	Jan 11, 2010	81	2010	steelhead correlation	5,475	2011	mark-recapture	275
2010	Jan 7, 2011	927	2011	mark-recapture	580	2012	mark-recapture	50,315
2011	Jan 11, 2012	355	2012	steelhead correlation	4,029	2013	mark-recapture	7,927
2012	Nov 29, 2012	199	2013	steelhead correlation	1,424	2014	mark-recapture	5,708
2013	Dec 31, 2013	2,752	2014	mark-recapture	16,961	2015	mark-recapture	7,253

Table 2. Annual abundance estimates of Shasta River spawners ($\hat{S}_t$), outmigrating parr ($\hat{J}_{t+1}$), and outmigrating smolts ($\hat{J}_{t+2}$) used to estimate freshwater productivity models. The dates on which the weir was removed and the methods used to estimate juvenile abundance are each listed.

Adult year	Weir removed	$\hat{S}_t$	Parr year	Estimation method	$\hat{J}_{t+1}$	Smolt year	Estimation method	$\hat{J}_{t+2}$
2004	Dec 9, 2004	373	2005	mark-recapture	15,581	2006	mark-recapture	10,833
2005	Dec 31, 2005	69	2006	mark-recapture	870	2007	steelhead correlation	1,178
2006	Dec 6, 2006	47	2007	steelhead correlation	2,837	2008	steelhead correlation	208
2007	Dec 15, 2007	249	2008	mark-recapture	1,457	2009	mark-recapture	5,396
2008	Dec 23, 2008	30	2009	steelhead correlation	5,423	2010	steelhead correlation	169
2009	Dec 22, 2009	9	2010	steelhead correlation	69	2011	mark-recapture	19
2010	Dec 17, 2010	44	2011	mark-recapture	2,177	2012	steelhead correlation	2,049
2011	Jan 7, 2011	62	2012	mark-recapture	3,446	2013	steelhead correlation	494
2012	Nov 30, 2012	115	2013	mark-recapture	1,930	2014	mark-recapture	850
2013	Dec 15, 2013	163	2014	mark-recapture	10,752	2015	mark-recapture	6,279

Table 3. Counts of adult Coho Salmon (*N*) observed at the Scott River, Shasta River, and Bogus Creek video counting weirs during years that were used to estimate models of adult migration timing. Weeks of weir operation are listed for each year and site.

	Scott River		Shasta River		Bogus Creek	
Year	Weeks of operation	*N*	Weeks of operation	*N*	Weeks of operation	*N*
2003	--	--	43 - 52	186	--	--
2004	--	--	42 - 49	371	43 - 49	405
2005	--	--	--	--	--	--
2006	--	--	41 - 48	83	43 - 52	46
2007	--	--	45 - 52	244	43 - 52	264
2008	41 - 52	62	43 - 51	137	42 - 52	137
2009	41 - 52	81	44 - 51	22	--	--
2010	40 - 52	929	43 - 50	48	40 - 50	176
2011	40 - 52	347	40 - 52	68	40 - 52	166
2012	40 - 49	200	41 - 48	126	40 - 52	198
2013	--	--	--	--	40 - 52	386
2014	40 - 49	489	41 - 49	60	40 - 52	131
2015	40 - 49	211	44 - 51	53	40 - 52	26

Table 4. Counts (*n*) of age-0^+ and age-1^+ Coho Salmon at the Scott River rotary screw trap and abundance estimates ($\widehat{N}$) in years that were used to estimate models of parr and smolt emigration timing. Weeks of trap operation and estimation methods are listed for each year and life stage.

		Age-0^+			Age-1^+		
Year	Weeks	*n*	Method	$\widehat{N}$	*n*	Method	$\widehat{N}$
2002	7 - 28	1,910	none	--	12	none	--
2003	7 - 28	281	none	--	1,412	mark-recapture	34,149
2004	7 - 27	58	none	--	91	none	--
2005	7 - 28	13,729	mark-recapture	80,498	248	mark-recapture	1,660
2006	8 - 28	276	mark-recapture	1,772	3,791	mark-recapture	75,097
2007	7 - 27	1,613	correlation	6,647	352	correlation	3,931
2008	7 - 26	925	mark-recapture	6,645	160	mark-recapture	941
2009	7 - 26	753	mark-recapture	3,899	5,302	mark-recapture	62,207
2010	7 - 26	678	correlation	5,475	185	correlation	2,174
2011	7 - 26	136	mark-recapture	556	78	mark-recapture	275
2012	7 - 26	647	correlation	4,029	2,904	mark-recapture	50,315
2013	7 - 26	372	correlation	1,424	627	mark-recapture	7,927
2014	7 - 26	1,565	mark-recapture	16,961	585	mark-recapture	5,708
2015	7 - 26	--	--	--	--	mark-recapture	7,253

Table 5. Counts (n) of age-0^+ and age-1^+ Coho Salmon at the Shasta River rotary screw trap and abundance estimates ($\widehat{N}$) in years that were used to estimate models of parr and smolt emigration timing. Weeks of trap operation and estimation methods are listed for each year and life stage.

		Age-0^+			Age-1^+		
Year	Weeks	n	Method	$\widehat{N}$	n	Method	$\widehat{N}$
2002	9 - 27	507	none	--	225	none	--
2003	7 - 27	292	none	--	2,432	mark-recapture	11,052
2004	7 - 26	388	mark-recapture	1,135	447	mark-recapture	1,799
2005	7 - 28	2,790	mark-recapture	14,263	407	mark-recapture	2,054
2006	7 - 28	199	mark-recapture	870	796	mark-recapture	10,833
2007	7 - 26	586	correlation	2,837	292	correlation	1,178
2008	7 - 26	384	mark-recapture	1,555	72	none	--
2009	7 - 26	725	correlation	5,423	1,770	mark-recapture	5,396
2010	7 - 26	13	correlation	69	35	correlation	169
2011	7 - 26	321	mark-recapture	2,160	4	correlation	19
2012	5 - 26	588	mark-recapture	3,446	395	correlation	2,049
2013	5 - 26	374	mark-recapture	1,930	152	correlation	494
2014	5 - 26	1,618	mark-recapture	10,752	299	mark-recapture	850
2015	5 - 26	189	mark-recapture	851	1,920	mark-recapture	6,279

Data sources: PIT tag monitoring

In recent years, YTFP, KDNR, and CDFW have monitored movement patterns of juvenile Coho Salmon implanted with PIT tags at trap sites and stationary interrogation arrays in the Klamath Basin. We selected observations of PIT tagged fish at several of these sites to inform models of overwinter survival and winter emigration rates, models of the timing of each major migration that juveniles undertake, and estimates of mainstem migration rates during the summer and winter redistributions. These sites were selected on the basis of data availability and are assumed to be representative of other Klamath River tributaries with naturally regulated flows. All observations were downloaded from the Klamath River Basin PIT tagging database. A summary of the basis for using these data sources to estimate models is provided in Table 6.

Overwinter survival and winter emigration ·

To estimate winter and spring emigration rates, we used observations collected at McGarvey Creek and Waukell Creek, two YTFP monitored sites in the lower Klamath Basin, and at Seiad Creek, a KDNR monitored site in the mid-Klamath Basin (Figure 2). Our dataset for estimating emigration rates was based on observations of age-0+ fish that were PIT tagged and released at a site during the intervening period (1 August to 31 October) between the summer and winter redistribution periods under the assumption that there was minimal emigration from a site during this period. We limited the dataset to years when more than 50 fish were tagged during this period. We generally classified fish that were last detected at a

Table 6. Sources of Klamath Basin PIT tag monitoring data used to estimate models of survival and migration timing.

Model	Site	Gear Types	Rationale
overwinter survival and winter emigration	McGarvey Creek	fyke net, stationary array	- extensive tagging effort during intervening period between summer and winter emigration periods in several years - stationary arrays with paired antennas enable inference of movement direction and detection probability - near continuous monitoring by stationary arrays during both winter and spring emigration periods in several years, which is necessary to jointly estimate survival and emigration rates
	Waukell Creek	fyke net, stationary array	
	Seiad Creek	fyke net, stationary array	
summer refuge entry timing	Panther Creek	fyke net, stationary array	- sites are non-natal, so all fish inhabiting them are immigrants - stationary arrays operated at entrance of each site, enabling continuous monitoring of immigrants - fyke nets enable monitoring of fish not tagged at other sites
	Waukell Creek	stationary array	
	Sandybar Floodplain Channel	fyke net, stationary array	
winter emigration timing	Seiad Creek	fyke net, stationary array	- sites appear to export many winter emigrants each year - extensive tagging upstream of stationary array in several years - near continuous monitoring by stationary arrays during winter in several years
	Sandybar Floodplain Channel	fyke net, stationary array	
winter refuge entry timing	Waukell Creek	fyke net, stationary array	- winter migration is primarily upstream at site, suggesting it receives many immigrants - located low in the Klamath Basin, so it is likely a destination for mid-Klamath emigrants - nearly daily sampling effort in winter in several years - continuous monitoring by stationary array in winter enables detection of fish tagged in other streams
smolt emigration timing	Panther Creek	stationary array	- sites all have stationary arrays located at the stream mouth - extensive tagging upstream of stationary array in some years - near continuous monitoring by stationary array during winter in some years - sites include both lower and mid-Klamath locations, thereby enabling basin location effects on timing to be quantified
	Waukell Creek	stationary array	
	McGarvey Creek	stationary array	
	Seiad Creek	stationary array	

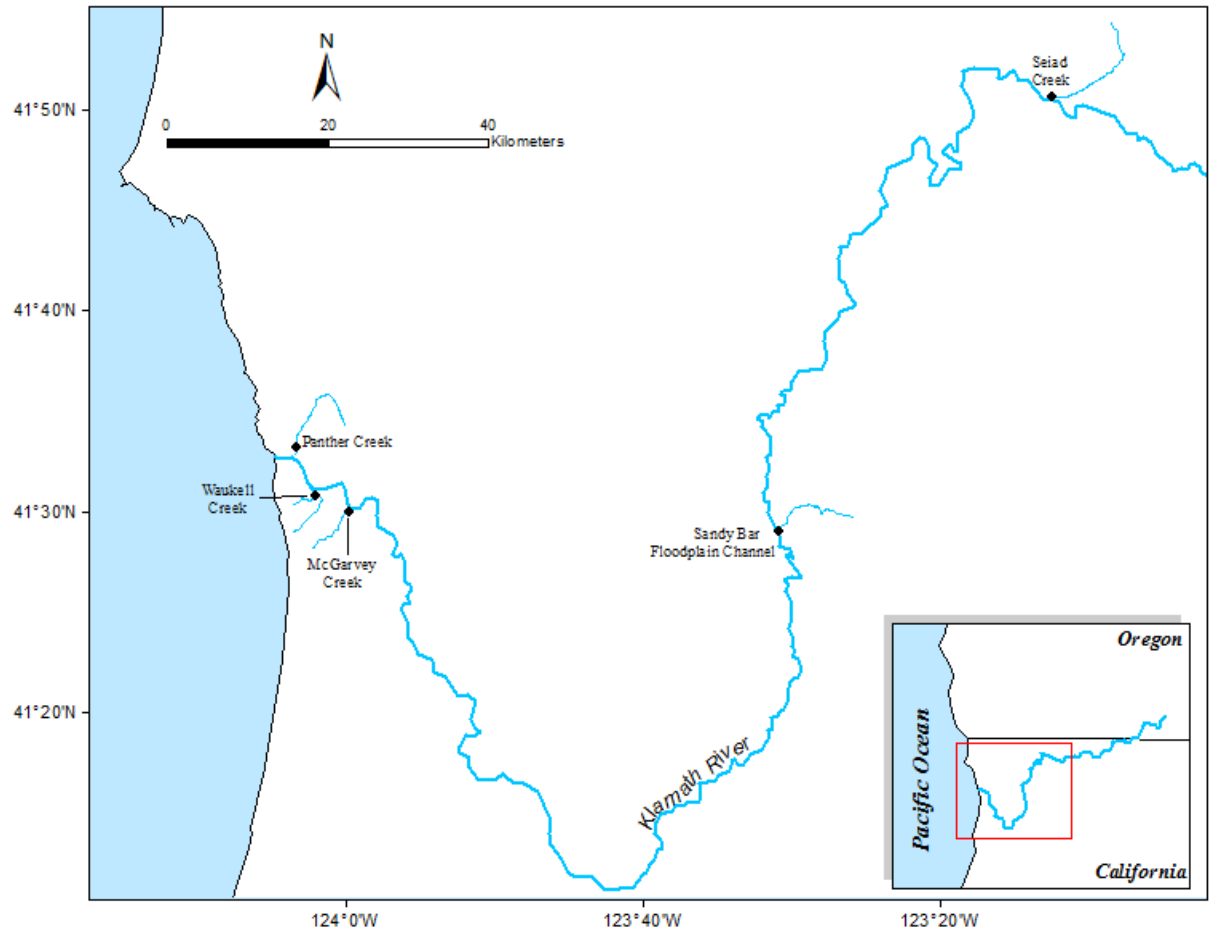

Figure 2. Map depicting locations of PIT tag monitoring sites in the Klamath Basin that were used to construct datasets for estimating models of overwinter survival and migration timing.

site between 1-November and 31-January as winter emigrants and fish that were last detected between 1-February and 30-June as spring emigrants.

McGarvey Creek is a small (third order), low gradient stream located at RKM 10.3 of the Klamath River. The stream supports runs of spawning Coho Salmon and provides rearing habitat for both natal and non-natal juveniles. Since 1997, YTFP has operated a pipe trap at RKM 1.9 of McGarvey Creek to capture downstream migrating juveniles. Auxiliary fyke nets have also been periodically operated in the lower reaches of McGarvey Creek to capture upstream migrants. Considerable efforts have been made to implant PIT tags into juveniles captured at these traps for the purpose of evaluating their movements. Movement during migration periods has been monitored by a stationary detection array, which was installed in lower McGarvey Creek at RKM 1.6 in November 2010. The array consists of an upstream antenna and another antenna that is positioned a short distance downstream, which provide a basis for inferring movement direction. Examination of detection histories

demonstrated that most fish (> 95%) that are detected at both antennas during the winter redistribution period and never again detected at McGarvey Creek are moving in a downstream direction, which suggests that they are emigrating from the system. To estimate winter emigration rates, we assumed that each of these fish were winter emigrants. We identified four brood years as suitable for estimating emigration rates at McGarvey Creek.

Waukell Creek is a small (third order) stream that enters the Klamath River at RKM 5.1 The lower reaches of the stream are characterized by a low gradient that likely provides high quality overwintering habitat for juvenile Coho Salmon. Furthermore, a section of Junior Creek, a tributary of Waukell Creek, forms a seasonal pond that provides suitable overwintering habitat. Monitoring of Waukell Creek has indicated that this stream is exclusively used by non-natal juveniles. Since 2006, a pair of fyke nets oriented in opposing directions to catch upstream and downstream migrating fish has been operated several days a week throughout the year, stream flows permitting. These traps have been used to conduct extensive PIT tagging of juvenile Coho Salmon for the purpose of monitoring their movement patterns. Monitoring of tagged fish has been accomplished through the operation of a stationary interrogation array, which was installed a short distance upstream of the fyke nets in December 2008. The array consists of two antennas that provide a basing for inferring movement direction. Examination of detection histories during winter demonstrated that fish are commonly detected numerous times at this array, which suggests that many fish rear in proximity to the array rather than migrating through. For those fish that exhibit clear movement patterns, the direction of movement is overwhelmingly upstream. Because of these characteristics, the assumption that we used to classify winter emigrants at McGarvey Creek is not reasonable for Waukell Creek and we therefore have little basis for estimating winter emigration rates in this stream. However, observations collected by fyke nets over a three-year period consistently demonstrated very little downstream movement in winter (Soto et al. 2016), which indicates that the winter emigration rate is typically close to zero in this stream. Hence, the spring emigration rate likely approximates the overwinter survival rate. We identified four brood years as suitable for estimating spring emigration rates at Waukell Creek.

Seiad Creek is a moderate sized tributary of the mid-Klamath Basin that enters the Klamath River at RKM 211.8. The stream supports runs of spawning Coho Salmon and provides rearing habitat for both natal and non-natal juveniles. Several traps, located on lower and upper Seiad Creek and in three constructed ponds, have been used by KDNR to PIT tag juvenile Coho Salmon. A stationary detection array has been continuously operated by KDNR on the lower end of Seiad Creek since January 2010, except when the system was damaged by high stream flows. This array initially consisted of three antennas positioned at distinct instream distances. Beginning in spring of 2011, operation of the upstream-most of these antennas ceased, reducing the Seiad Creek array to a two-antenna array for subsequent migration periods. Examination of detections histories at the array have indicated that most fish (> 95%) that are detected there in winter and never detected again at Seiad Creek are moving downstream. For the purpose of estimating winter emigration rates, we assumed that all of these fish were winter emigrants. We identified four brood years as suitable for estimating emigration rates at Seiad Creek.

Summer refuge entry timing ·

We evaluated factors that govern the time at which parr enter thermal refuges during summer redistribution events with data collected from PIT tagged fish at two lower Klamath Basin tributaries (Panther Creek and Waukell Creek) and at a floodplain channel fed by Sandy Bar Creek in the mid-Klamath Basin (Figure 2). Fyke nets have been used to sample upstream migrating parr in the lower reaches of Panther Creek and Waukell Creek and parr migrating into the Sandy Bar floodplain channel. Additionally, a stationary PIT array has been concurrently operated at each of these sites during some survey years, thereby providing a means of remotely monitoring the migration of fish that were tagged in other locations. Unlike other tributaries to the Klamath River, Coho Salmon do not spawn in these creeks, and sampled juveniles are non-natal fish that have migrated from another tributary in the Klamath Basin. Therefore, these sites provide an excellent opportunity to evaluate environmental factors that cue parr to leave the mainstem Klamath River and enter thermal refugia during summer redistributions. The majority of parr that migrate into these sites in summer have not yet been tagged and are therefore observed for the first time on their tagging date. The extent of sampling effort at these sites has varied considerably from year to year, ranging from biweekly to daily. To ensure adequate and consistent coverage within years, we limited the dataset for the summer refuge entry model to years in which near daily sampling effort was maintained from May through August. These criteria led to the creation of a dataset that included five summer redistribution periods among the three refuges (Table 7).

Table 7. Number of age-0^+ Coho Salmon (*N*) observed at fyke nets and stationary PIT arrays in the Klamath Basin from 1 May to 18 August in each year. These data were used to fit models of refuge entry timing during the summer redistribution period.

Site	Gear ID	Type	Latitude	Longitude	Year	*N*
Panther Creek	PantherCrkU	Fyke net	41.5536	-124.0569	2011	117
	PantherCrkB1	Stationary array	41.5537	-124.0569	2011	18
Waukell	WaukellCrkLowerU	Fyke net	41.5133	-124.0358	2008	81
					2010	108
					2011	266
	WaukellCrkA1	Stationary array	41.5130	-124.0353	2008	0
					2010	2
					2011	1
Sandy Bar	Sandy Bar Floodplain Channel	Fyke net	41.4866	-123.5175	2008	320
	Sandy Bar Floodplain Channel	Stationary array	41.4866	-123.5175	2008	0

Winter emigration timing ·

We evaluated factors governing emigration timing of parr during the winter redistribution period with data collected from PIT tagged fish in the Sandy Bar floodplain channel and in Seiad Creek (Figure 2). These sites were selected because they appear to export large numbers of emigrants during winter each year and because they have been extensively monitored during the winter emigration period in several years. In recent years, extensive efforts have been made to tag parr inhabiting these rearing sites prior to the overwintering period and to monitor the movement of tagged fish during the overwintering period with stationary PIT arrays. The Sandy Bar floodplain channel has been intensively monitored with multiple antennas since summer of 2008. Because of the number of antennas and their arrangement in the channel, tagged fish that occupy the site are often detected hundreds of times during residency. Fish that cease to be detected for several days are seldom detected again, which indicates that the last detection date of a fish marks its date of death or emigration. Seiad Creek is monitored with a stationary PIT array located on the lower end of the creek. The array has been continuously operated since January 7, 2010, except during periods when high flows caused outages. Examination of data collected at the array indicates that fish that are detected there are likely emigrating from the stream (Soto et al. 2016). We selected the years of 2010-2012 to fit models of winter emigration timing based on the large numbers of parr that were tagged from 1 August and 31 October, the intervening period between the summer and winter redistribution periods, in those years. These tagged parr were assumed to occupy each site at the beginning of the winter redistribution period, which we define as 1 November to 31 January. While some last detections may correspond to fish that had died, for the purpose of characterizing environmentally driven patterns in winter emigration timing we assumed that tagged fish that were last detected at each site during the overwintering period were winter emigrants. The dataset used to fit the winter emigration model included six winter redistribution periods between the two sites (Table 8).

Table 8. Number of age-0^+ Coho Salmon (N_t) tagged at monitoring sites from 1 July to 31 October and number of emigrants detected at stationary arrays (N_d) from 1 November to 31 January each year. Data were used to fit models of emigration timing during the winter redistribution period.

		Tagging events		Detection events		
Year	Site	Gear ID	N_t	Gear ID	Period	N_d
2010-11	Seiad Creek	Seiad Creek Lower	773	Seiad Creek Ant 1	1 Nov - 5 Jan	85
		Seiad Creek Upper	117			
2011	Seiad Creek	Karuk Site at Seiad Creek Alexander Pond	174	Seiad Creek Ant 1	1 Nov - 31 Dec	58
		Karuk Site at Seiad Creek Harold and Annie's	36			
		Seiad Creek Lower	254			
2012	Seiad Creek	Caltrans Pond (aka Lower Seiad Pond)	289	Seiad Creek Ant 1	1 Nov - 5 Dec	59
		Karuk Site at Seiad Creek Alexander Pond	229			
		Canyon Creek	30			
		Seiad Creek Lower beaver ponds	391			
2010-11	Sandy Bar	Sandy Bar Floodplain Channel	164	Sandy Bar Floodplain Channel Ant 1	1 Nov - 31 Jan	138
		Sandy Bar Floodplain Channel Backwater	200			
2011	Sandy Bar	Sandy Bar Floodplain Channel	120	Sandy Bar Floodplain Channel Ant 1	1 Nov - 31 Dec	247
		Sandy Bar Floodplain Channel Backwater	390			
2012	Sandy Bar	Sandy Bar Floodplain Channel	243	Sandy Bar Floodplain Channel Ant 1	1 Nov - 20 Dec	136

Winter refuge entry timing ·

We evaluated factors that determine refuge entry timing of parr during the winter redistribution period with data collected from PIT tagged fish at Waukell Creek (Figure 2). Sampling of parr in this stream with an upstream oriented fyke net has demonstrated that this site is likely a destination for many parr that enter from the mainstem Klamath River in winter. We selected data from monitoring of brood years 2007 to 2011 to fit the upstream movement model because near daily sampling effort was maintained during the winter redistribution period in each of these. Further, a stationary PIT array was continuously operated near the mouth of Waukell Creek during each of these years, thereby providing a means of detecting immigrants that had been PIT tagged in other streams. The dataset used to estimate the model of winter refuge entry timing included five winter redistribution periods at Waukell Creek (Table 9).

Smolt emigration timing ·

We evaluated factors that determine spring emigration timing of smolts with data collected at stationary PIT arrays located at three lower Klamath Basin tributaries (Panther Creek, Waukell Creek, and McGarvey Creek) and at Seiad Creek, a middle Klamath Basin tributary (Figure 2). We limited the model estimation dataset to include only years when the array at a site was continuously operated throughout the emigration period and to include only the last detection of each individual fish at an array under the assumption that emigration occurred soon after the last detection. These criteria led to the creation of a dataset that include fourteen smolt emigration periods among the four tributaries (Table 10).

Table 9. Number of age-0^+ Coho Salmon (*N*) observed at fyke nets and stationary PIT arrays in Waukell Creek from 22 October to 11 February in each year. These data were used to fit models of refuge entry timing during the winter redistribution period.

Site	Gear ID	Type	Latitude	Longitude	Year	*N*
Waukell	WaukellCrkLowerU	Fyke net	41.5133	-124.0358	2008-09	858
					2009-10	240
					2010-11	785
					2011-12	682
					2012-13	80
	WaukellCrkA1	Stationary array	41.5130	-124.0353	2008-09	104
					2009-10	67
					2010-11	118
					2011-12	125
					2012-13	306

Table 10. Number of age-1^{+} Coho Salmon (*N*) detected at stationary arrays in the Klamath Basin during the smolt emigration period each year. Data were used to fit models of smolt emigration timing.

Stream	Gear ID	Latitude	Longitude	Period	Year	*N*
Panther Creek	PantherCrkB1	41.5536	-124.0570	17 March - 19 June	2009	74
					2010	184
					2011	165
					2012	190
					2013	158
Waukell Creek	WaukellCrkA1	41.5130	-124.0355	12 March - 29 June	2009	878
					2010	209
					2011	299
					2012	441
McGarvey Creek	McGarveyCrkLower1	41.5004	-123.9977	12 March - 29 June	2011	232
Seiad Creek	Seiad Creek Ant 1	41.8437	-123.2075	15 February - 9 June	2010	115
					2011	220
					2012	197
					2013	244

Data sources: environmental data

The models of freshwater productivity and migration timing evaluated suites of environmental covariates that were drawn from a variety of data sources. We estimated daily photoperiods (time between sunrise and sunset) with the geosphere package (Hijams 2016) in R (R Core Team, 2016). We obtained measurements of daily water temperature in gauged tributaries and in the mainstem Klamath River from surveys conducted by the U.S. Forest Service and U.S. Fish and Wildlife Service. In tributaries where measurements were missing, we used a non-linear model based on gridded meteorological data (Mohseni et al. 1998) to estimate daily mean stream temperatures. We downloaded measurements of daily discharge from U.S. Geological Survey operated gages in the Scott River (11519500), the Shasta River (11517500), and at several sites in the Klamath River (11530500, 11523000, 11520500, and 11516530) from http://waterdata.usgs.gov/nwis/dv. Measurements of daily discharge in Bogus Creek were provided by Pacific Power from 2012-2015 (Demian Ebert; personal communication). We estimated daily discharge in ungauged tributaries based on drainage-area proportionate allocation of the discharge differential recorded at Klamath River gauges upstream and downstream of a tributary.

Statistical methods: freshwater productivity

Ricker model of productivity ·

We explored the freshwater population dynamics of Coho Salmon in the Scott and Shasta Rivers by analyzing the relationship between abundances of adult spawners and abundances of emigrant parr and smolts from the resulting year class. To quantify this relationship for each life stage we fit a Ricker Model of the form

$$R_{l,t} = \alpha_{l,t} S_{l,t} e^{-\beta_{l,t} S_{l,t} + \varepsilon} \ , \quad (1)$$

where $R_{l,t}$ is the estimated abundance of juvenile Coho Salmon from life stage *l* emigrating from tributary *t*, $S_{l,t}$ is the estimated the number of spawners that produced them, $\alpha_{l,t}$ is the intrinsic productivity of the life stage in the tributary, $\beta_{l,t}$ is a term capturing potential density-dependent production of the life stage, and ε is a residual error term with mean 0 and standard deviation σ. The Ricker model can be expressed in linear form as

$$\ln(R_{l,t}) = \ln(\alpha_{l,t}) + \ln(S_{l,t}) - \beta_{l,t} S_{l,t} + \varepsilon \ , \quad (2)$$

thereby enabling the parameters to be estimated with standard linear models. The linear model is fit as

$$\ln(R_{l,t}) = \theta_0 + \ln(S_{l,t}) + \theta_S S_{l,t} + \varepsilon \ , \quad (3)$$

where $\alpha_{l,t} = \exp(\theta_0)$, $\beta_{l,t} = -\theta_S$, and $\ln(S_{l,t})$is coded as an offset. The linearized Ricker model readily accommodates environmental covariates as

$$\ln(R_{l,t}) = \theta_0 + \ln(S_{l,t}) + \theta_S S_{l,t} + \sum \theta_j x_j + \varepsilon \ , \quad (4)$$

where x_j is the j^{th} covariate and θ_j is the slope of the j^{th} covariate. We estimated linear models of this form with the *lme4* package (Bates et al 2015) in R (R Core Team 2016). We evaluated combinations of environmental covariates that were of hypothetical importance to the production of each life stage by using an information theoretic approach, based on Akaike's Information Criterion (AIC), to identify the suite of covariates that minimized the information loss and therefore represented the most parsimonious model. We quantified the relative probability, P_R,, that the i^{th} model minimized the information loss as

$$P_R = exp\left(\frac{AIC_{min} - AIC_i}{2}\right) , \quad (5)$$

where the lowest AIC score observed among all models was AIC_{min} (Burnham and Anderson 2002).

Bayesian estimates of model parameters ·

We quantified the statistical uncertainty of the parameters of the best-fit model from each life stage and river by estimating each model under a Bayesian framework. We drew samples from the posterior distribution of each parameter with the Markov chain Monte Carlo (MCMC) algorithm, which was performed in R by using the package *rjags* (Plummer 2016) to call JAGS (Plummer 2003) from R. We constrained the prior for θ_s to a biologically realistic range of -1 to 0, and used non-informative and proper priors for θ_0 and each j^{th} environmental covariate,

$$\theta_s \sim U(-1, 0) \quad (6)$$

$$\theta_0, \theta_j \sim N(0, 1 \text{ x } 10^{-3})$$

We ran each model for 200,000 iterations with a burn-in period of 100,000 and used a thinning interval of 10 to reduce autocorrelation among posterior samples. We tested convergence with the Gelman-Rubin convergence diagnostic $\hat{R}$ (Gelman and Rubin 1992) which compared variance within and between chains.

Covariates of parr abundance ·

The abundance of emigrant parr is likely a function of habitat accessibility for spawning adults and environmental stressors that trigger early emigration from the Scott and Shasta Rivers in spring. To evaluate these processes, we identified a suite of covariates that accounted for stream conditions during the adult migration and parr emigration periods (Table 11). Low discharge during spawning migrations (Figures 3, 4) may prevent adults from accessing small tributaries that likely contain some of the most favorable spawning habitat in each river system, thereby forcing adults to spawn in the mainstem. To evaluate the effect of low discharge, we computed the average annual discharge of each tributary from 1 November to 15 December of year *t* to overlap the typical extent of spawning activity. We evaluated high temperatures and low discharge in spring as potential triggers of early emigration from the Scott River by computing the mean temperature and discharge from 1 April to 30 June of year *t* + 1. We standardized each environmental covariate, x_j, as

$$f(x_j) = \frac{x_j - \mu_j}{\sigma_j} \ , \qquad (7)$$

where μ_j and σ_j are the mean and standard deviation of covariate x_j over its time series.

Covariates of smolt abundance ·

The abundance of emigrant smolts is determined by the productivity of adult spawners and the survival of juveniles through smoltification. To evaluate these processes, we evaluated a suite of covariates that accounted for stream conditions during the adult migration and during the freshwater rearing stage (Table 11). The selection of these covariates was based on the general life history of Coho Salmon in the Klamath River (Lestelle 2007). As in the parr abundance model, we evaluated the mean stream discharge during the adult migration period as a model covariate under the expectation that low flows in the Scott and Shasta Rivers would adversely affect productivity by precluding access to favorable spawning tributaries. We constructed two additional covariates to evaluate the potentially deleterious effects of high summer temperatures and high winter stream flows on parr survival. We estimated an index of summer thermal stress as the number of days from 1 June to 15 September of year *t* + 1 on which the mean stream temperature exceeded 20 ˚C to overlap the period where parr redistribute in response to rapidly increasing water temperatures (Figures 3, 4), and we estimated an index of winter discharge as the mean discharge from 1 December in year *t* + 1 to 31 January in year *t* + 2 to overlap the period of heightened winter discharge (Figures 3, 4). We standardized each environmental covariate as in equation 7.

Table 11. Definitions of covariates evaluated in Ricker models of abundance of emigrant parr and smolts in the Scott and Shasta Rivers.

Model	Term	Variable definition
Parr	θ_{QM}	Mean discharge during adult migration period, 1 November to 15 December of year *t*
	θ_{QV}	Mean discharge during spring, 1 April to 30 June in year *t* + 1
	θ_{TV}	Mean temperature during spring, 1 April to 30 June in year *t* + 1
Smolt	θ_{QM}	Mean discharge during adult migration period, 1 November to 15 December of year *t*
	θ_{TS}	Days from 1 June to 15 September of year *t* + 1 when temperature exceeded 20 ˚C
	θ_{QW}	Mean discharge during winter, 1 December of year *t* + 1 to 31 January of year *t* + 2

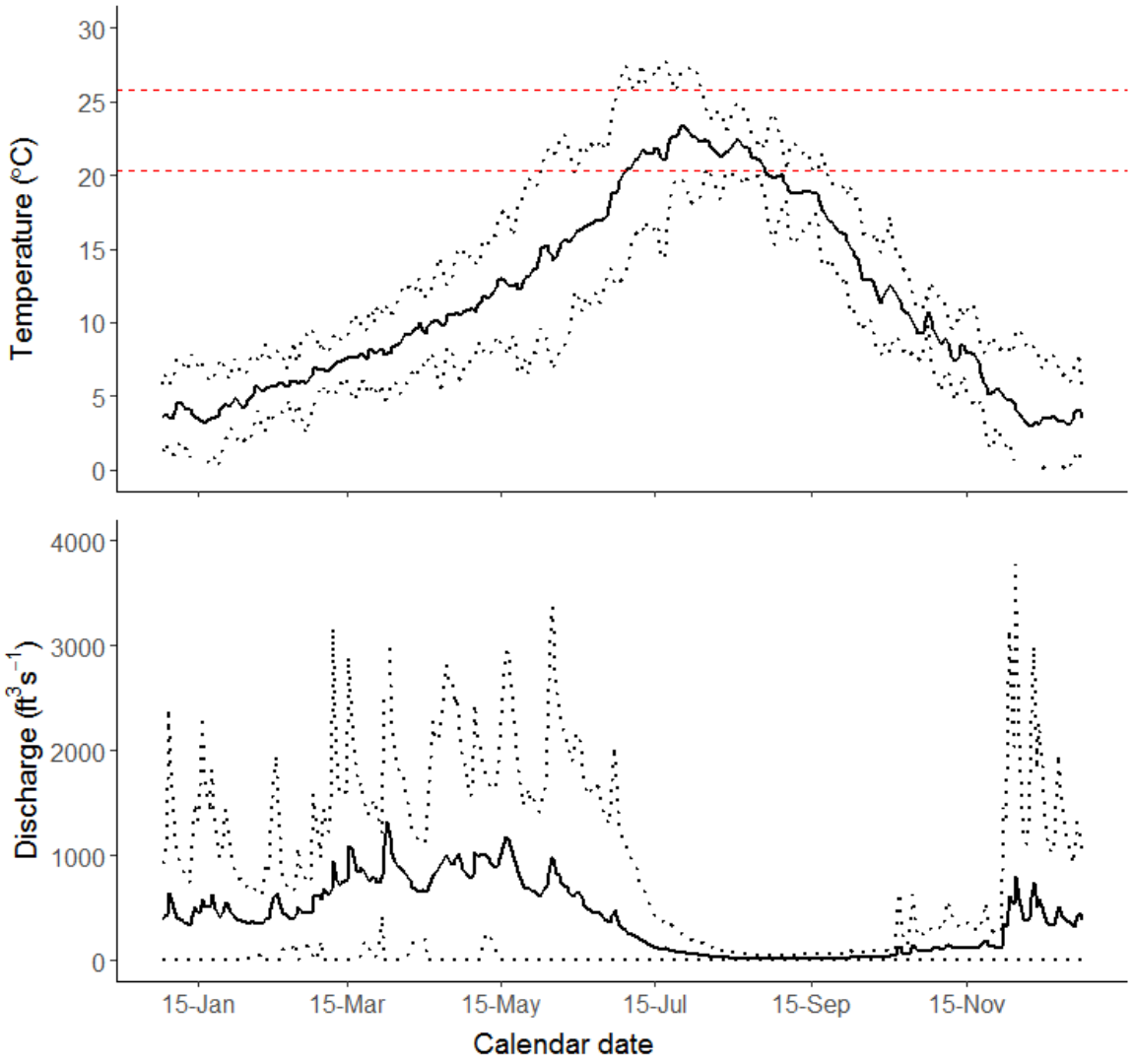

Figure 3. Daily means (solid lines) and 95% prediction intervals (broken lines) of temperature (top panel) and discharge (bottom panel) in the Scott River from 2007-2015. Broken, red lines at 20.3 ˚C and 25.8 ˚C mark potential temperatures where cessation of growth (Brett 1952) and mortality (Beschta et al 1988) occur in Coho Salmon, respectively.

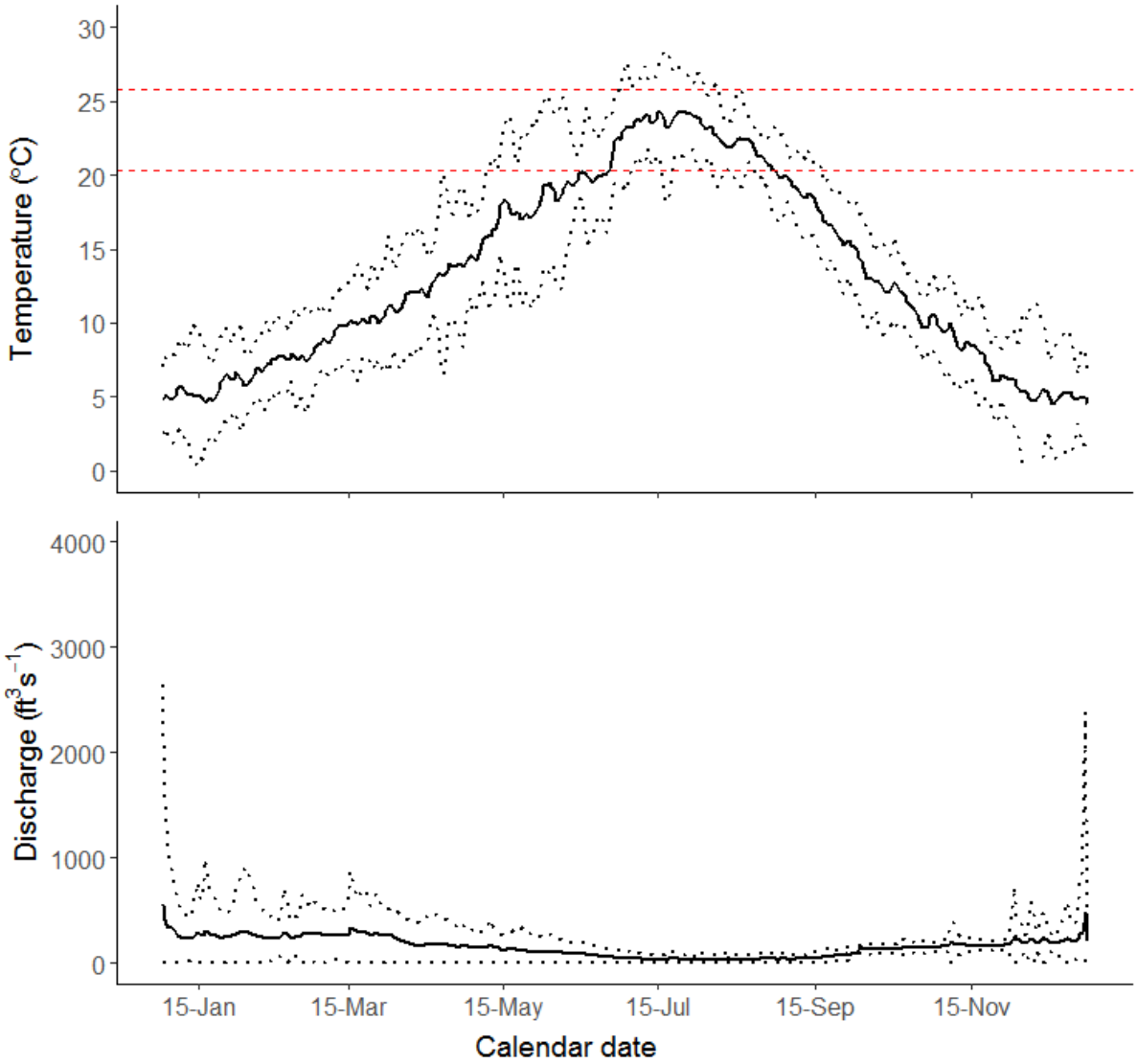

Figure 4. Daily means (solid lines) and 95% prediction intervals (broken lines) of temperature (top panel) and discharge (bottom panel) in the Shasta River from 2004-2015. Broken, red lines at 20.3 ˚C and 25.8 ˚C mark potential temperatures where cessation of growth (Brett 1952) and mortality (Beschta et al 1988) occur in Coho Salmon, respectively.

Statistical methods: overwinter survival and winter emigration

Detection efficiencies and emigration rates ·

Each of the stationary PIT arrays chosen for estimating models of overwinter survival and winter emigration rates was configured in a way that enabled us to estimate its detection efficiency. We estimated the detection efficiencies, the proportion of tagged fish that were detected leaving the site during the winter redistribution period (i.e. the winter emigration rate), and the proportion that were detected leaving the site during the smolt emigration period (i.e. the spring emigration rate) with a Bayesian multistate mark-recapture model. The model consisted of two likelihoods: a primary likelihood to estimate the emigration rates and a secondary likelihood to estimate the detection efficiencies. The primary likelihood, p^1, was comprised of the probabilities that a fish was not detected, detected in winter, or detected in spring (denoted by subscripts '0', '1', and '2', respectively)

$$p_0^1 = [1 - \phi_w - \phi_s] + [\phi_w * (1 - p_w)] + [\phi_s * (1 - p_s)] \quad (8)$$

$$p_1^1 = \phi_w * p_w$$

$$p_2^1 = \phi_s * p_s$$

$$y \sim Mult(p^1, N_t),$$

where ϕ_w and ϕ_s are the winter and spring emigration rates and p_w and p_s are the winter and spring detection efficiencies. We assumed that the frequencies of N_t tagged fish with each capture history, y, followed a multinomial distribution.

The secondary likelihood, p^2, was comprised of the probabilities of each possible detection history, given that a fish was detected at the array. For a two-antenna array, the secondary likelihood was

$$p_{01}^2 = \frac{(1 - p_1) * p_2}{p} \quad (9)$$

$$p_{10}^2 = \frac{p_1 * (1 - p_2)}{p}$$

$$p_{11}^2 = \frac{p_1 * p_2}{p}$$

$$p = 1 - (1 - p_1) * (1 - p_2)$$

where the p_1 is the seasonal (winter or spring) detection efficiency of the upstream antenna, p_2 is the seasonal detection efficiency of the downstream antenna, and p is their combined seasonal efficiency. The detection efficiencies of these antennas were assumed to be independent. For a three-antenna array, the secondary likelihood was

$$p_{001}^2 = \frac{(1 - p_1) * (1 - p_2) * p_3}{p} \quad (10)$$

$$p_{010}^2 = \frac{(1-p_1) * p_2 * (1-p_3)}{p}$$

$$p_{011}^2 = \frac{(1-p_1) * p_2 * p_3}{p}$$

$$p_{100}^2 = \frac{p_1 * (1-p_2) * (1-p_3)}{p}$$

$$p_{101}^2 = \frac{p_1 * (1-p_2) * p_3}{p}$$

$$p_{110}^2 = \frac{p_1 * p_2 * (1-p_3)}{p}$$

$$p_{111}^2 = \frac{p_1 * p_2 * p_3}{p}$$

$$p = 1 - (1-p_1) * (1-p_2) * (1-p_3)$$

We assumed that the seasonal frequencies of N_d detected fish with each detection history, *y*, followed a multinomial distribution,

$$y \sim Mult(p^2, N_d) \quad \textbf{(11)}$$

We assigned vague beta priors to the seasonal detection efficiency of the i^{th} antenna and to each emigration rate,

$$p_i \sim Beta(1,1) \quad \textbf{(12)}$$

$$\phi \sim Beta(1,1)$$

The estimated emigration rates correspond to the joint probability that a fish survived and exhibited one of two migratory behaviors. To partition survival from migratory behavior we derived three additional parameters, the annual survival rate (S), the monthly survival rate (S_m), and the probability of winter migratory behavior (Ψ_w), as

$$S = \phi_w + \phi_s \quad \textbf{(13)}$$

$$S_m = S^{1/t}$$

$$\Psi_w = \frac{\phi_w}{S_m^{t_w}},$$

where t is the mean residence time (i.e. the number of months between the tagging date and final detection date) of all detected emigrants and t_w is the mean residence time of detected winter emigrants.

We ran each model for 400,000 iterations with a burn-in period of 300,000, and used a thinning interval of 10 to reduce autocorrelation among posterior samples. We tested convergence with the Gelman-Rubin convergence diagnostic, $\hat{R}$.

Statistical methods: migration timing

Logistic mixed effects model ·

We used a seven-day time step to estimate models of the timing of the adult and smolt migrations and of each of the migrations that comprise the summer and winter redistributions. We selected this time interval over a daily time step to reduce the frequency of observations where zero fish were counted, a condition known as 'sparseness' (McCullagh and Nelder 1989). We constructed migration timing models of all life stages under a previously detailed analytical framework (Spence and Dick 2014). Specifically, we fit abundances of migrating fish per interval to generalized linear mixed models where we assumed that the abundance of migrant fish observed during the i^{th} interval (n_i) of a migration period followed a binomial distribution,

$$n_i \sim Bin(N_i, p_i)\ , \qquad \textbf{(14)}$$

where N_i is the estimated number of potential emigrants or immigrants, defined as the annual number of migrants observed or estimated at a site during the corresponding migration period minus the cumulative number of migrants through interval $i - 1$, and p_i is the migration probability. We assumed that migration probabilities during each interval were independent and conditional on a vector of explanatory variables, x_i, and expressed the logit-transformed migration probabilities (l_i) as a linear combination of explanatory variables plus an observation-level random effect, ε_i,

$$l_i = log\left(\frac{p_i}{1 - p_i}\right) = x_i\beta + \varepsilon_i \qquad \textbf{(15)}$$

$$\varepsilon_i \sim N(0, \sigma^2).$$

The inclusion of an observation-level random effect allowed for overdispersion, thereby reducing the likelihood of underestimating the standard errors. We estimated the coefficients of the linear predictor ($\boldsymbol{\beta}$) and the variance of the random effect (σ^2) with the *lme4* package (Bates et al. 2015) in R.

To determine the most parsimonious model that could be constructed from environmental data, we used an information theoretic approach based on AIC to select the suite of covariates and interactions that minimized the information loss and, therefore, comprised the most parsimonious model. Model parsimony was expressed as the likelihood that a given model minimized the information loss, P_R, as described in equation 5.

Covariates of adult migration timing ·

We selected a suite of covariates to evaluate the effects of photoperiod, temperature, and discharge on adult migration timing in the Scott River, the Shasta River, and in Bogus Creek (Table 12). The selection of these covariates was based on the general life history of Klamath River Coho Salmon (Lestelle 2007). We calculated daily mean values of each of these variables over weekly intervals, and calculated the mean discharge and temperature near the mouth of the Klamath River during September, the historical month of peak Coho Salmon entry into the Klamath River (Weitkamp et al. 1995), to evaluate whether

environmentally mediated entry into the mainstem subsequently influenced tributary entry time. Scott and Shasta River hydrographs indicated that pulses of adults tend to occur during weeks of rapidly increasing discharge. To account for this pattern, we constructed a covariate reflecting change in discharge (ΔQ_{max}) observed in each week. Next, based on evaluations of hydrographs, we chose a threshold value of ΔQ_{max} of 0.1 to identify weeks where discharge increased substantially. Finally, we classified each week as a 'flood' week if ΔQ_{max} exceeded the threshold or a 'calm' week otherwise. This resulted in a two-level categorical variable. We standardized covariates P_i, T^*, and Q^* as described in equation 7. We standardized covariates T_i and Q_i as deviations from their historical weekly means to alleviate multicollinearity with P_i

$$f(x_j) = \frac{x_j - \mu_{ij}}{\sigma_{ij}} , \quad \textbf{(16)}$$

where μ_{ij} and σ_{ij} are the mean and standard deviation of covariate x_j in the i^{th} week over the time series.

Covariates of parr emigration timing in the Scott and Shasta Rivers ·

We selected a suite of covariates to evaluate the effects of adult migration timing, incubation temperatures, and environmental stressors on parr emigration timing in the Scott and Shasta Rivers (Table 12). We jointly accounted for potential effects of adult migration timing and incubation temperatures on parr emigration timing by computing the sum of daily temperatures (accumulated temperature units, ATUs) from the median adult migration date to the beginning of the i^{th} week. We evaluated two environmental stressors that may cue early emigration of parr, high stream temperatures and low stream flows, by computing weekly means and maximum weekly changes for each of these variables. We standardized continuous covariates as deviations from their overall means as described in equation 7.

Covariates of smolt emigration timing in the Scott and Shasta Rivers ·

To model smolt emigration timing in the Scott and Shasta Rivers, we selected a suite of covariates to evaluate the effects of photoperiod, temperature, and discharge (Table 12). We calculated daily means of these variables over weekly intervals, and we calculated the mean stream temperature during the first six weeks of each year to evaluate whether temperatures prior to emigration explained variation in migration probabilities. Scott River hydrographs indicated that pulses of smolts tended to follow weeks of where discharge decreased substantially. To account for this pattern, we constructed a covariate corresponding to change in discharge by first identifying the maximum decrease in discharge over a three-day period, ΔQ_{max}, observed in each week. Next, based on examinations of hydrographs, we chose a threshold value of ΔQ_{max} of 1,000 cfs to identify weeks with notable decreases in discharge. Finally, to account for delayed migratory responses of up to one week, we classified each week as an 'ebb' week if it or the previous week exceeded the threshold or a 'calm' week otherwise. The result was a two-level categorical variable. Shasta River hydrographs indicated that the smolt emigration generally peaked following dramatic declines in discharge at the start of the irrigation season. To account for this pattern, we defined irrigation periods as weeks when the mean discharge of the Shasta River was less

than 200 cfs. We then constructed a two-level categorical variable indicating whether the i^{th} week occurred during an irrigation period. We standardized continuous covariates as deviations from their overall means as described in equation 7.

Covariates of summer refuge entry timing ·

We evaluated the effects of temperature and discharge on the time at which parr entered thermal refuges during the summer redistribution period using several covariates (Table 13). We calculated the mean temperature and discharge recorded at nearby Klamath River gauges during each seven-day interval to evaluate whether daily environmental variation in the mainstem was involved in cueing refuge entry. We also calculated the maximum increase in temperature and maximum decrease in discharge observed at nearby mainstem gauges during each interval to evaluate the role of changing environmental conditions in cueing refuge entry. We standardized each of these covariates as deviations from their overall means as described in equation 7.

Covariates of winter emigration timing ·

We selected a suite of covariates to evaluate the effects of discharge on the time at which parr emigrated from rearing sites during the winter redistribution period (Table 13). We estimated the mean discharge at each site during seven-day intervals to evaluate whether daily environmental variation in discharge was involved in cueing emigration events. Hydrographs indicated that pulses of parr tended to occur on days where discharge increased substantially. To account for this pattern, we constructed a covariate corresponding to change in discharge by first calculating the maximum proportionate change in discharge over a three day period, ΔQ_{max} , that occurred within each seven-day interval. Next, based on examinations of hydrographs, we chose a threshold value of $\Delta Q_{max} \geq 1.0$ to identify intervals with substantial increases in discharge. Finally, we classified each interval as a 'flood' interval if ΔQ_{max} exceeded the threshold or a 'calm' interval otherwise. We also included the interval number as a covariate to evaluate whether the response to discharge was time dependent. We standardized continuous covariates as described in equation 7.

Covariates of winter refuge entry timing ·

The effect of discharge on the time at which migrating parr entered Waukell Creek during the winter redistribution period was evaluated using several covariates (Table 13). We calculated the mean discharge recorded near the mouth of the Klamath River during each seven-day interval to evaluate whether daily variation in discharge was involved in cueing refuge entry. Hydrographs indicated that parr tended to migrate into Waukell Creek on days where discharge increased substantially. We quantified this pattern by computing a two-level categorical variable denoting whether an interval occurred during a 'flood' event or 'calm' event in the same manner described for the winter emigration timing covariates. We also included the interval number as a covariate to evaluate whether the response to

Table 12. Definitions of main effect terms and rationales for interaction terms evaluated in models of the timing of the adult migration, parr emigration, and smolt emigration in the Scott River, Shasta River, and Bogus Creek.

Model	Main term	Variable definition
Adult migration	P_i	Mean photoperiod (hours between sunrise and sunset) during the i^{th} interval
	T^*	Mean temperature recorded near the Klamath River mouth during September
	T_i	Mean tributary temperature during the i^{th} interval
	Q^*	Mean discharge recorded near the Klamath River mouth during September
	Q_i	Mean tributary discharge during the i^{th} interval
	F_i	Categorical variable denoting whether the i^{th} interval was during a 'flood' event
Parr emigration	ATU_i	Accumulated temperature units at the beginning of the i^{th} interval
	Q_i	Mean tributary discharge during the i^{th} interval
	ΔQ_i	Maximum decrease in tributary discharge during the i^{th} interval
	T_i	Mean tributary temperature during the i^{th} interval
	ΔT_i	Maximum increase in tributary temperature during the i^{th} interval
Smolt emigration	P_i	Mean photoperiod (hours between sunrise and sunset) during the i^{th} interval
	T_i	Mean tributary temperature during the i^{th} interval
	T	Mean tributary temperature during the first six weeks of the year
	Q_i	Mean tributary discharge during the i^{th} interval
	E_i	Categorical variable denoting whether the i^{th} interval was during an 'ebb' event
	I_i	Categorical variable denoting whether the i^{th} interval was during an irrigation period

Model	Interaction term	Rational
Adult migration	P_i x T_i	Response to temperature may be time dependent
	P_i x Q_i	Response to discharge may be time dependent
	P_i x F_i	Response to 'flood' events may be time dependent
Parr emigration	ATU_i x Q_i	Response to discharge may be time dependent
	ATU_i x ΔQ_i	Response to change in discharge may be time dependent
	ATU_i x T_i	Response to temperature may be time dependent
	ATU_i x ΔT_i	Response to change in temperature may be time dependent
Smolt emigration	P_i x T_i	Response to temperature may be time dependent
	P_i x E_i	Response to 'ebb' events may be time dependent
	P_i x I_i	Response to irrigation may be time dependent

discharge patterns was time dependent. We standardized weekly mean discharge as described in equation 7.

Covariates of smolt emigration timing ·

Variation in smolt emigration probability, in tributaries with naturally regulated flow patterns, was evaluated according to covariates describing photoperiod, temperature, and discharge (Table 13). To evaluate the effect of location on emigration timing, we constructed a two-level categorical variable denoting whether a tributary was located in the lower or middle portion of the Klamath Basin. We calculated the mean photoperiod and mean stream temperature during each interval to evaluate migratory responses of smolts to daily environmental variation. We also calculated the mean stream temperature during the first six weeks of each year to evaluate whether temperatures prior to emigration were involved in priming smolts for emigration. Hydrographs indicated that pulses of smolts tended to follow days where discharge increased substantially. To account for this pattern, we constructed a covariate corresponding to change in discharge by first calculating the maximum proportionate change in discharge over a one-day period, ΔQ_{max}, that occurred within each seven-day interval. As was done in the winter emigration and entry timing models, we chose a threshold value of $\Delta Q_{max} \geq 1.0$ to identify intervals with substantial increases in discharge and classified each interval as a 'flood' interval if ΔQ_{max} exceeded the threshold or a 'calm' interval otherwise. We standardized continuous covariates as described in equation 7.

Model predictive performance ·

We evaluated the predictive performance of each migration model by comparing frequencies of model-predicted migrants to frequencies of migrants observed at monitoring sites over each migration period. The number of fish residing in a tributary or in the mainstem that had yet to migrate at the beginning of the i^{th} interval of a migration period was N_i. For the first interval of each period, we set N_i equal to N, the annual number of observed migrants. To estimate the number of fish that migrated during the i^{th} interval, (1) the logit probability, l_i, was predicted as a linear function of the environmental factors and associated coefficients from the most parsimonious migration model; (2) the probability of migrating, p_i, was estimated by back-transforming the logit probability,

$$p_i = \frac{\exp(l_i)}{1 + exp(l_i)} \ ; \qquad (17)$$

(3) p_i was multiplied by N_i to give n_i, the number of migrants; and (4) n_i was subtracted from N_i to give N_{i+1}. We repeated this procedure for each interval to estimate frequency distributions of migrants during the adult migration, parr emigration, summer redistribution, winter redistribution, and smolt emigration periods. We constructed bar plots to compare model-predicted frequencies of migrants to observed frequencies.

Table 13. Definitions of main effect terms and rationales for interaction terms evaluated in models of the timing of four Coho Salmon migratory events: summer refuge entry, winter emigration, winter refuge entry, and spring emigration.

Model	Main term	Variable definition
Summer refuge entry	T_i^*	Mean Klamath River temperature measured at a nearby gauge during the i^{th} interval
	ΔT_i^*	Maximum daily increase in Klamath River temperature during the i^{th} interval
	Q_i^*	Mean Klamath River discharge measured at a nearby gauge during the i^{th} interval
	ΔQ_i^*	Maximum daily decrease in Klamath River discharge during the i^{th} interval
Winter emigration	I_i	Interval number
	Q_i	Mean tributary discharge estimated at a location during the i^{th} interval
	F_i	Categorical variable for whether a tributary experienced a 'flood' event during the i^{th} interval
Winter refuge entry	I_i	Interval number
	Q_i^*	Mean Klamath River discharge measured at a nearby gauge during the i^{th} interval
	F_i^*	Categorical variable for if the Klamath R. experienced a 'flood' event during the i^{th} interval
Spring emigration	P_i	Mean photoperiod (hours between sunrise and sunset) during the i^{th} interval
	K	Categorical variable for whether a tributary is in the lower or middle KRB
	T	Mean tributary temperature during the first six weeks of the year
	T_i	Mean tributary temperature during the i^{th} interval
	F_i	Categorical variable for whether a tributary experienced a 'flood' event during the i^{th} interval
Model	**Interaction term**	**Rational**
Winter emigration	I_i x Q_i	Response to tributary discharge may be time dependent
	I_i x F_i	Response to tributary 'flood' events may be time dependent
Winter refuge entry	I_i x Q_i^*	Response to Klamath River discharge may be time dependent
	I_i x F_i^*	Response to Klamath River 'flood' events may be time dependent
Spring emigration	K x P_i	Response to photoperiod may be location specific
	P_i x F_i	Response to tributary 'flood' events may be time specific

Statistical methods: mainstem migration rates

Two critical periods of the life history of Klamath Basin Coho Salmon occur when juveniles seek refuge from rising stream temperatures during summer and rising stream flows during winter. During these redistribution periods, many juveniles are thought to use the mainstem Klamath River as a migratory corridor to access tributaries and off-channel habitats that provide favorable thermal or hydraulic conditions. The specific refuge that a given fish enters is likely an outcome of its mainstem migration rate, seasonal changes in water conditions in the mainstem, and the habitat suitability of the refuge. To quantify mainstem migration rate, we used the extensive network of PIT-tag arrays that have been operated in the Klamath Basin in recent years to identify mainstem movement events. We constructed capture histories of age-0^+ fish from May through August to overlap the summer redistribution period and from November through January to overlap the winter redistribution period. The capture histories revealed many instances where a fish was observed at two different locations in the Klamath Basin and where transit between those locations necessitated migration in the mainstem Klamath River. We constructed separate

datasets from pairs of observations collected during the summer and winter redistribution periods (Tables 14 and 15) and estimated migration rate, r, as

$$r = {}^{L}/_{t}\,, \qquad \textbf{(18)}$$

where *L* is the in-river length (km) between the locations where a fish was observed and *t* is the number of days separating the observations. We limited the dataset to paired observations where $L \geq 10$ and fit the resulting summer and winter datasets to log-normal distributions with the *MASS* package (Venables and Ripley 2002) in R.

To jointly account for the mean downstream movement rate of a group of fish (advection) and the magnitude of spreading within that group (diffusion), we used an advection-diffusion model (Zabel and Anderson 1997). The model specifies that the probability density function for the travel time distribution of a cohort of fish originating at the same time and point of origin and migrating to the same destination is given by

$$g(t) = \frac{L}{\sqrt{2\pi\sigma^2 t^3}} exp\left(\frac{-(L-rt)^2}{2\sigma^2 t}\right), \qquad \textbf{(19)}$$

where *t* is the travel time, *L* is the distance separating the points of origin and destination, *r* is the mean migration rate, and σ is the diffusion rate. To estimate *r* and σ with our dataset, which consisted of fish that originated at different times and points of origin and migrated to different destinations, we numerically maximized the log likelihood of this equation by substituting the travel distances and times of individual fish into it,

$$-\sum_{i=N}^{i} log_e\left[\frac{L_i}{\sqrt{2\pi\sigma^2 t_i^3}} exp\left(\frac{-(L_i - rt_i)^2}{2\sigma^2 t_i}\right)\right]. \qquad \textbf{(20)}$$

To account for seasonal differences in travel times we expressed *r* and σ as linear functions of dummy variables, corresponding to whether the season was summer ('0') or winter ('1'),

$$r = \alpha_r + \beta_r Season \qquad \textbf{(21)}$$

$$\sigma^2 = (\alpha_\sigma + \beta_\sigma Season)^2\ ,$$

and estimated the values of α and β that maximized the likelihood of the data.

Table 14. Paired observations (*n*) of age-0^+ Coho Salmon at PIT-tag monitoring sites in the Klamath Basin from 1 May to 31 August. Observations were used to estimate mainstem migration rates (*r*, km/day) in summer based on the distance (*L*) between each pair of monitoring sites. In-river distances (rkm) denote the distance of a site from the mouth of the Klamath River.

Upstream		Downstream				
Site	rkm	Site	rkm	*L*	*n*	*r*
Shasta River	289.0	Seiad Creek	211.8	77.2	17	10.42
		Cade Creek	178.0	111.0	1	6.94
		Klamath - Bulk Plant	176.7	112.3	1	9.98
		Waukell Creek	5.1	283.9	1	11.57
Klamath - Kinsmen Trap	237.5	Seiad Creek	211.8	25.7	2	3.53
Tom Martin Creek	232.1	West Grider Creek	212.3	19.8	1	1.33
		Seiad Creek	211.8	20.3	3	5.70
		Titus Creek	155.6	76.5	1	8.50
O'Neil Creek	223.5	Seiad Creek	211.8	11.7	3	1.32
Seiad Creek	211.8	Titus Creek	155.6	56.2	2	2.19
		Aiken's Creek	78.5	133.3	1	5.13
Fort Goff Creek	206.1	Cade Creek	178.0	28.1	1	11.43
Titus Creek	155.6	Klamath - Sandy Bar	124.7	30.9	2	1.25
		Waukell Creek	5.1	150.5	1	10.88
Klamath - Sandy Bar	124.7	Aiken's Creek	78.5	46.2	1	1.80
		Salt Creek	1.2	123.5	1	4.16
Aiken's Creek	78.5	Panther Creek	1.3	77.2	1	1.76

Table 15. Paired observations (*n*) of juvenile Coho Salmon at PIT-tag monitoring sites in the Klamath Basin from 1 November to 31 January. Observations were used to estimate mainstem migration rates (*r*, km/day) in winter based on the distance (*L*) between each pair of monitoring sites. In-river distances (rkm) denote the distance of a site from the mouth of the Klamath River.

Upstream		Downstream				
Site	rkm	Site	rkm	*L*	*n*	*r*
Horse Creek	240.2	Klamath - Bulk Plant	176.7	63.5	1	3.00
		Klamath - Sandy Bar	124.7	115.5	2	5.48
		McGarvey Creek	10.3	229.9	2	10.75
		Waukell Creek	5.1	235.1	2	8.89
		Panther Creek	1.3	238.9	3	9.43
Tom Martin Creek	232.1	Seiad Creek	211.8	20.3	1	0.39
		McGarvey Creek	10.3	221.8	1	4.97
Seiad Creek	211.8	Klamath - Bulk Plant	176.7	35.1	14	6.72
		Boise Creek	90.0	121.8	1	10.15
		McGarvey Creek	10.3	201.5	5	8.77
		Waukell Creek	5.1	206.7	2	20.47
		Panther Creek	1.3	210.5	10	16.76
Elk Creek	171.9	Waukell Creek	5.1	166.8	1	7.94
		Panther Creek	1.3	170.6	1	5.19
Titus Creek	155.6	Klamath - Sandy Bar	124.7	30.9	4	13.5
		Klamath - Stanshaw Pool	123.7	31.9	2	29
		McGarvey Creek	10.3	145.3	2	6.55
		Waukell Creek	5.1	150.5	2	3.78
Dillon Creek	137.1	Waukell Creek	5.1	132.0	2	4.40
Teep Teep Creek	131.1	Waukell Creek	5.1	126.0	1	9.00
Klamath - Sandy Bar	124.7	McGarvey Creek	10.3	114.4	13	21.31
		Waukell Creek	5.1	119.6	33	19.19
		Panther Creek	1.3	123.4	3	24.52
Klamath - Stanshaw Pool	123.7	McGarvey Creek	10.3	113.4	1	4.40
		Waukell Creek	5.1	118.6	6	8.10
		Panther Creek	1.3	122.4	1	3.24
Camp Creek	92.1	McGarvey Creek	10.3	81.8	3	2.89
		Waukell Creek	5.1	87.0	8	3.06
		Panther Creek	1.3	90.8	1	2.22
Klamath - Big Bar RST	81.8	Waukell Creek	5.1	76.7	4	8.21
		Panther Creek	1.3	80.5	3	11.31
Aiken's Creek	78.5	McGarvey Creek	10.3	68.2	1	3.39
		Waukell Creek	5.1	73.4	14	3.73
		Panther Creek	1.3	77.2	3	6.02

Results

Freshwater productivity

Ricker models of Scott River abundance ·

Annual estimates of adult Coho Salmon abundance varied substantially in the Scott River (63 - 2,752 fish) over the seven-year time series. We estimated Ricker models of parr and smolt abundance with all possible combinations of environmental covariates. The model of Scott River parr abundance with the lowest AIC (Table 16) included discharge during the adult migration period, discharge during spring, and temperature during spring, each of which exhibited a negative, linear relationship with the residuals from the parr abundance model (Figure 5). The effect of temperature was not consistent with expectations and so we selected the model with next lowest AIC (P_R = 0.287), which differed by its exclusion of temperature, as the best-fit model. The Scott River smolt abundance model with the lowest AIC (Table 17) included temperature during summer and discharge during winter, each of which exhibited a negative, linear relationship with the residual errors (Figure 5). The model with the next lowest AIC, which differed by its inclusion of discharge during the adult migration, was not as well supported (P_R = 0.375). The Ricker model provided some evidence of density-dependence in the relationship between spawner and parr abundance, but this pattern was driven by only two data points (Figure 6). Conversely, the Ricker model provided minimal evidence of density-dependence in the relationship between spawner and smolt abundance (Figure 6). Together, abundance of spawners and the environmental covariates from the best-fit models accounted for a large portion of the interannual variation in both parr (R^2 = 0.879) and smolt (R^2 = 0.957) abundance. The Bayesian analysis estimated posterior means of the best-fit model parameters which approximated their respective maximum likelihood estimates (Table 18).

Table 16. Coefficients and standard errors (parentheses) of standardized covariates evaluated in Ricker models of emigrant parr abundance in the Scott River. Models are sorted according to their relative probability (P_R) of being the most parsimonious. Covariates are defined as follows: θ_S, spawner abundance; θ_{QM}, discharge during adult migration; θ_{QV}, vernal discharge; θ_{TV}, vernal temperature.

AIC	P_R	θ_0	θ_S	θ_{QM}	θ_{QV}	θ_{TV}
14.032	--	3.384 (0.285)	-1.4 E-4 (2.4 E-4)	-1.058 (0.238)	-2.920 (1.621)	-2.147 (1.600)
16.527	0.287	3.362 (0.320)	-1.3 E-4 (2.7 E-4)	-1.182 (0.247)	-0.768 (0.266)	
18.780	0.093	3.332 (0.375)	-1.3 E-4 (3.1 E-4)	-1.225 (0.290)		0.704 (0.309)
23.823	0.007	3.090 (0.515)	-1.0 E-4 (4.1 E-4)	-1.216 (0.416)		
28.736	0.001	3.256 (0.763)	-1.2 E-4 (6.4 E-4)		-5.725 (4.021)	-4.899 (3.927)
29.607	< 0.001	-0.827 (0.676)	-1.1 E-4 (6.7 E-4)		-0.827 (0.676)	
29.833	< 0.001	2.856 (0.806)	-7.5 E-4 (6.4 E-4)			
30.349	< 0.001	3.089 (0.846)	-1.0 E-4 (7.0 E-4)			0.685 (0.704)

Table 17. Coefficients and standard errors (parentheses) of standardized covariates evaluated in Ricker models of smolt abundance in the Scott River. Models are sorted according to their relative probability (P_R) of being the most parsimonious. Covariates are defined as follows: θ_S, spawner abundance; θ_{QM}, discharge during adult migration; θ_{QV}, vernal discharge; θ_{TV}, vernal temperature.

AIC	P_R	θ_0	θ_s	θ_{QM}	θ_{TS}	θ_{QW}
15.036	--	3.051 (0.275)	-2.5 E-4 (2.2 E-4)		-0.476 (0.226)	-1.091 (0.223)
16.999	0.375	3.045 (0.342)	-2.5 E-4 (2.8 E-4)	0.039 (0.386)	-0.482 (0.282)	-1.066 (0.369)
19.383	0.114	3.132 (0.371)	-3.5 E-4 (2.9 E-4)			-0.980 (0.296)
21.295	0.044	3.146 (0.431)	-3.6 E-4 (3.5 E-4)	-0.094 (0.483)		-1.044 (0.472)
26.055	0.004	3.077 (0.604)	-2.8 E-4 (4.8 E-4)	0.649 (0.487)		
26.495	0.003	2.981 (0.634)	-1.7 E-4 (5.2 E-4)	0.789 (0.529)	-0.453 (0.524)	
26.624	0.003	3.202 (0.641)	-4.3 E-4 (5.1 E-4)			
28.383	0.001	3.170 (0.710)	-3.9 E-4 (5.7 E-4)		-0.213 (0.570)	

Table 18. Posterior means, standard errors, and 95% Bayesian credible intervals (BCI) of coefficient estimates for standardized covariates from the best-fit models of emigrant parr and smolt abundance in the Scott River. Covariates are defined as follows: θ_S, spawner abundance; θ_{QM}, discharge during adult migration; θ_{QV}, vernal discharge; θ_{TV}, vernal temperature.

Model	Parameter	Mean	SE	95% BCI	Sample
Parr	θ_0	3.417	0.776	2.108 – 5.068	19000
	θ_s	-1.408 E-3	0.617 E-3	-2.763 E-3 – -0.405 E-3	21000
	θ_{QM}	-1.193	0.623	-2.382 – -0.031 E-3	30000
	θ_{QV}	-0.789	0.662	-2.132 – 0.398 E-3	30000
Smolt	θ_0	3.207	0.598	2.363 – 4.525	21000
	θ_s	-0.436 E-3	0.444 E-3	-1.510 E-3 – -0.024 E-3	6500
	θ_{TS}	-0.436	0.530	-1.349 – 0.608	12000
	θ_{QW}	-1.071	0.526	-2.027 – -0.069	29000

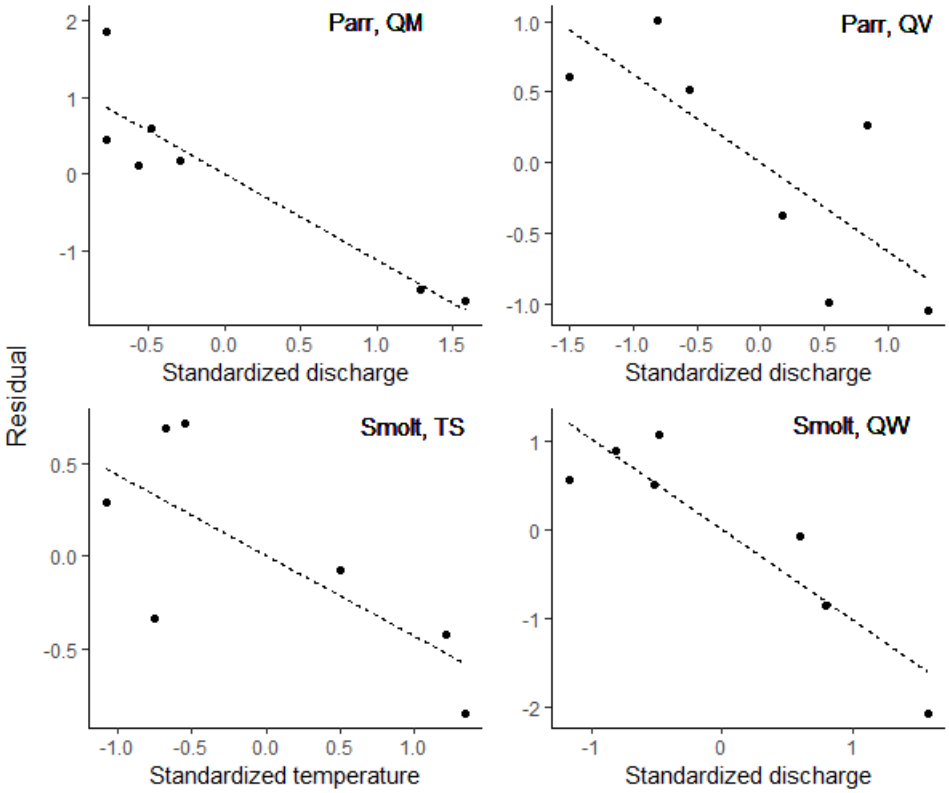

Figure 5. Univariate plots depicting the relationship between residuals from the Ricker models of parr and smolt abundance in the Scott River and each of the best supported standardized covariates. Covariates include discharge during the adult migration (*QM*), discharge during spring (*QV*), temperature during summer (*TS*), and discharge during winter (*QW*).

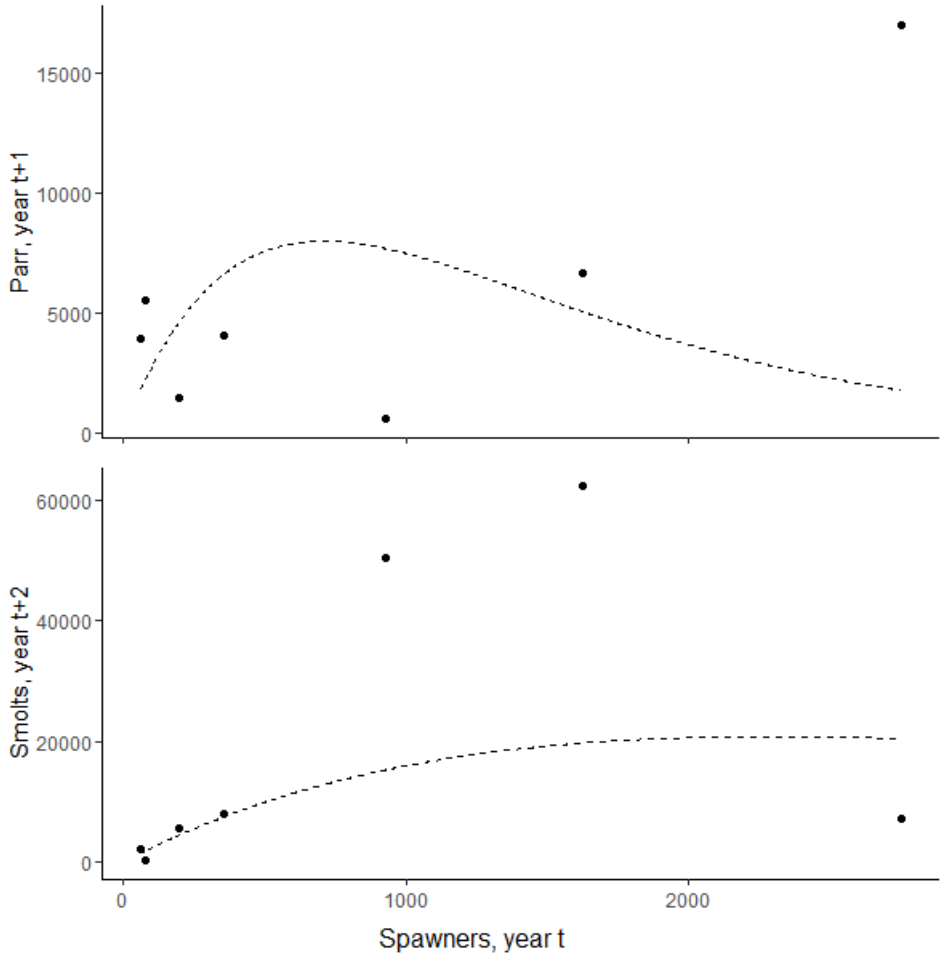

Figure 6. Relationship between the abundance of spawners and the abundances of emigrant parr (top panel) and smolts (bottom panel) in the Scott River. Fitted values from the Ricker model of each life stage are depicted by a broken line.

Ricker models of Shasta River abundance ·

Annual estimates of adult Coho Salmon abundance varied substantially in the Shasta River (9 - 373 fish) over the ten-year time series. We estimated Ricker models of parr and smolt abundance with all possible combinations of environmental covariates. The model of Shasta River parr abundance with the lowest AIC only included spawner abundance (Table 19). The model with the next lowest AIC, which differed by its inclusion of discharge during the adult migration, was not as well supported (P_R = 0.392). The model of Shasta River smolt abundance with the lowest AIC only included spawner abundance (Table 20). The model with the next lowest AIC, which differed by its inclusion of discharge during the adult migration, was not as well supported (P_R = 0.417). Collectively, there was minimal support for effects of environmental covariates on parr or smolt production in the Shasta River. The Ricker model provided minimal evidence of a density-dependent relationship between spawner abundance and either parr or smolt abundance (Figure 7). The abundance of adults accounted for a modest amount of the interannual variation in parr abundance (R^2 = 0.433)

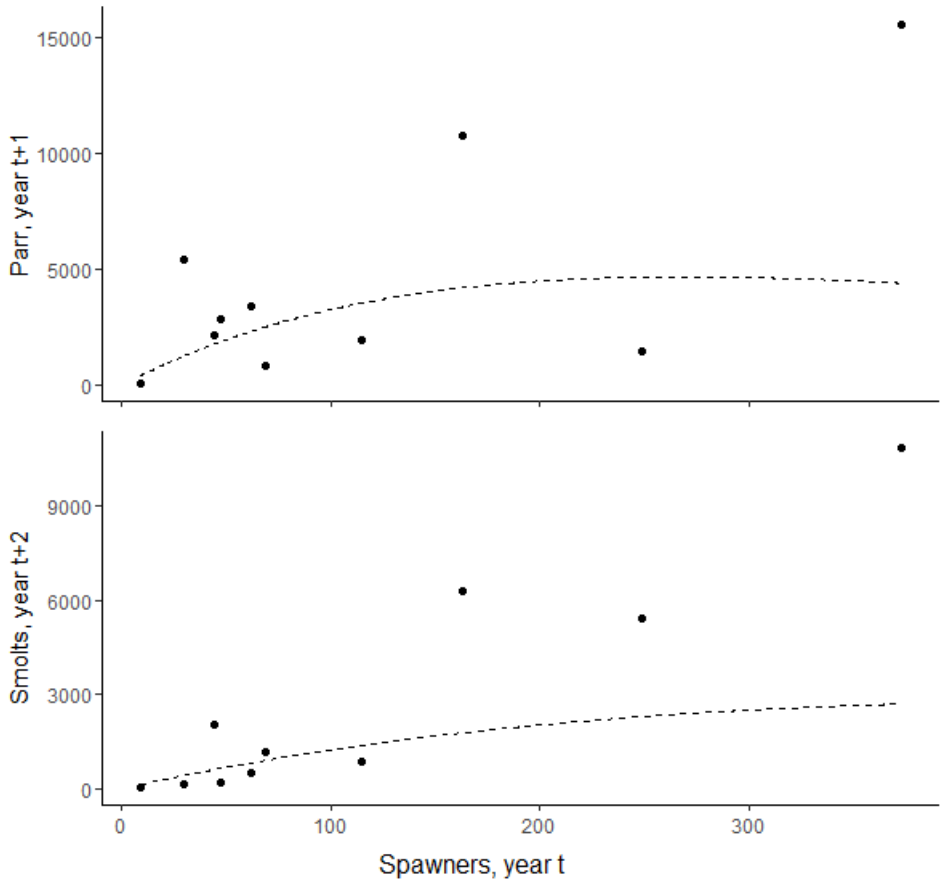

Figure 7. Relationship between the abundance of spawners and the abundances of emigrant parr (top panel) and smolts (bottom panel) in the Shasta River. Fitted values from the Ricker model of each life stage are depicted by a broken line.

Table 19. Coefficients and standard errors (parentheses) of standardized covariates evaluated in Ricker models of emigrant parr abundance in the Shasta River. Models are sorted according to their relative probability (P_R) of being the most parsimonious. Covariates are defined as follows: θ_S, spawner abundance; θ_{QM}, discharge during adult migration; θ_{QV}, vernal discharge; θ_{TV}, vernal temperature.

AIC	P_R	θ_0	θ_S	θ_{QM}	θ_{QV}	θ_{TV}
34.789	--	3.604 (0.526)	-1.5 E-3 (3.3 E-3)			
36.663	0.392	3.577 (0.566)	-1.3 E-3 (3.6 E-3)	-0.123 (0.414)		
36.350	0.458	3.636 (0.553)	-1.8 E-3 (3.5 E-3)		-0.225 (0.402)	
36.060	0.530	3.591 (0.543)	-1.4 E-3 (3.4 E-3)			0.286 (0.392)
38.301	0.173	3.674 (0.634)	-2.1 E-3 (4.2 E-3)	0.115 (0.670)	-0.311 (0.661)	
37.915	0.210	3.564 (0.590)	-1.2 E-3 (3.7 E-3)	-0.127 (0.431)		0.287 (0.421)
37.975	0.203	3.610 (0.589)	-1.6 E-3 (3.7 E-3)		-0.111 (0.489)	0.232 (0.484)
39.909	0.077	3.542 (0.742)	-1.0 E-3 (5.2 E-3)	-0.177 (0.971)	0.064 (1.098)	0.319 (0.713)

Table 20. Coefficients and standard errors (parentheses) of standardized covariates evaluated in Ricker models of smolt abundance in the Shasta River. Models are sorted according to their relative probability (P_R) of being the most parsimonious. Covariates are defined as follows: θ_S, spawner abundance; θ_{QM}, discharge during adult migration; θ_{QV}, vernal discharge; θ_{TV}, vernal temperature.

AIC	P_R	θ_0	θ_s	θ_{QM}	θ_{TS}	θ_{QW}
30.149	--	1.911 (0.417)	4.9 E-3 (2.6E-3)			
31.899	0.417	1.941 (0.446)	4.7 E-3 (2.8 E-3)	0.137 (0.326)		
31.967	0.403	1.906 (0.442)	5.0 E-3 (2.8 E-3)		-0.115 (0.320)	
31.466	0.518	1.692 (0.532)	6.8 E-3 (3.8 E-3)			-0.309 (0.440)
33.605	0.178	1.940 (0.475)	4.7 E-3 (3.0 E-3)	0.167 (0.354)	-0.147 (0.346)	
32.722	0.276	1.664 (0.555)	7.0 E-3 (4.0 E-3)	0.240 (0.353)		-0.421 (0.487)
32.573	0.298	1.555 (0.579)	8.0 E-3 (4.2 E-3)		-0.271 (0.362)	-0.484 (0.511)
32.299	0.341	1.413 (0.580)	9.2 E-3 (4.3 E-3)	0.427 (0.378)	-0.457 (0.391)	-0.803 (0.574)

and a large amount of the variation in smolt abundance (R^2 = 0.781). The Bayesian analysis estimated posterior means of the best-fit model parameters which approximated their respective maximum likelihood estimates in most instances (Table 21). The primary departure was in the estimate of θ_S in the smolt abundance model, for which the maximum likelihood estimate was positive and the posterior mean was negative. This discrepancy was likely the result of constraints we placed on the prior for this parameter.

Overwinter survival and winter emigration

We used a multistate mark-recapture model to estimate overwinter survival and winter emigration rates over a four-year period at each of three tributaries (Table 22). The Waukell Creek data limited us to estimating spring emigration rates only. The detection probability in spring at Waukell Creek was consistently high, ranging between 0.88 and 0.99. The model estimated annual apparent survival rates at this site that ranged between 0.29 and 0.56 and monthly apparent survival rates that ranged between 0.79 and 0.91. If we assume that winter emigration rates are close to zero in this stream, as has been indicated by migrant trapping efforts (Soto et al. 2016), these apparent survival rates are close to true survival rates. In McGarvey Creek, detection probabilities were consistently high, ranging between 0.90 and 0.96 in winter and 0.81 and 0.99 in spring. The model estimated annual survival rates in McGarvey Creek that ranged between 0.23 and 0.49, monthly survival rates that ranged between 0.78 and 0.89, and winter emigration rates that ranged between 0.19 and 0.44. In Seiad Creek, detection probabilities were generally close to 0.90; the two lowest detection probabilities were observed in winter of 2012 (p_w = 0.30) and in spring of 2011 (p_s = 0.77). The model estimated annual survival rates at Seiad Creek that ranged between 0.37 and 0.57, monthly survival rates that ranged between 0.79 and 0.91, and winter emigration rates that ranged between 0.20 and 0.31. However, significant antenna outages during migration periods likely influenced our estimates of these rates in all but 2010. The standard errors of the estimated survival and emigration rates were generally less than 0.05 and many instances were close to 0.01, which indicated that we estimated these rates with high precision.

Table 21. Posterior means, standard errors, and 95% Bayesian credible intervals (BCI) of coefficient estimates for standardized covariates from the best-fit models of emigrant parr and smolt abundance in the Shasta River.

Model	Parameter	Mean	SE	95% BCI	Sample
Parr	θ_0	3.859	0.560	2.864 – 5.091	30000
	θ_s	-3.724 E-3	2.902 E-3	-10.772 E-3 – -0.170 E-3	30000
Smolt	θ_0	2.706	0.524	1.764 – 3.861	8900
	θ_s	-1.953 E-3	2.078 E-3	-7.445 E-3 – -0.050 E-3	30000

Table 22. Numbers of juvenile Coho Salmon PIT tagged during fall (N_f) and detected emigrating the following winter (N_w) and spring (N_s) at three streams in the Klamath Basin. Emigrants were detected at stationary PIT-tag interrogation arrays. Standard errors (parentheses) are listed for the winter and spring detection efficiencies (p_w and p_s), winter and spring emigration rates (Φ_w and Φ_s), annual and monthly survival rates (S and S_m), and winter emigrant proportion (Ψ_w). Estimates of Φ_s at Waukell Creek were assumed to be close to S, given the low winter emigration rates observed there. Highlighted estimates were likely influenced by antenna outages.

	Tagging		Winter emigration			Spring emigration			Derived parameters		
Stream	Year	N_f	N_w	p_w	Φ_w	N_s	p_s	Φ_s	S	S_m	Ψ_w
Waukell	2008	525	--	--	--	173	0.99 (0.01)	0.33 (0.02)	0.33 (0.02)	0.82 (0.01)	--
	2009	86	--	--	--	38	0.96 (0.03)	0.46 (0.06)	0.46 (0.06)	0.86 (0.02)	--
	2010	522	--	--	--	271	0.93 (0.03)	0.56 (0.03)	0.56 (0.03)	0.91 (0.01)	--
	2011	390	--	--	--	98	0.88 (0.03)	0.29 (0.03)	0.29 (0.03)	0.79 (0.01)	--
McGarvey	2010	286	76	0.92 (0.03)	0.29 (0.03)	56	0.99 (0.01)	0.20 (0.02)	0.49 (0.03)	0.87 (0.01)	0.44 (0.04)
	2011	123	17	0.90 (0.06)	0.16 (0.04)	35	0.81 (0.09)	0.36 (0.07)	0.52 (0.07)	0.89 (0.02)	0.24 (0.05)
	2012	381	32	0.99 (0.01)	0.09 (0.01)	55	0.99 (0.01)	0.15 (0.02)	0.23 (0.02)	0.78 (0.01)	0.19 (0.03)
	2013	321	32	0.96 (0.03)	0.11 (0.02)	79	0.83 (0.05)	0.30 (0.03)	0.41 (0.04)	0.85 (0.01)	0.19 (0.03)
Seiad	2009	560	--	--	--	170	0.99 (0.01)	0.30 (0.02)	--	--	--
	2010	696	81	0.89 (0.03)	0.13 (0.01)	234	0.77 (0.04)	0.44 (0.03)	0.57 (0.04)	0.91 (0.01)	0.20 (0.02)
	2011	482	62	0.99 (0.01)	0.13 (0.02)	100	0.87 (0.03)	0.24 (0.02)	0.37 (0.03)	0.79 (0.01)	0.24 (0.03)
	2012	727	39	0.30 (0.12)	0.22 (0.12)	136	0.89 (0.03)	0.21 (0.02)	0.43 (0.12)	0.87 (0.03)	0.31 (0.12)

Migration timing

Adult migration timing in the Scott River, Shasta River, and Bogus Creek ·

We estimated generalized linear mixed models of weekly adult migration probabilities in the Scott River, Shasta River, and Bogus Creek with most combinations of covariates and included interactions where a sufficient rationale supported them. We assumed photoperiod was the primary determinant of adult migration time and therefore included it in every model, and we excluded several combinations of covariates that exhibited multicollinearity. Observations of discharge at Bogus Creek were only available from 2012-2015. Models fit with data from these years produced little evidence of an effect of either metric of Bogus Creek discharge (Q_i, $P = 0.29$; ΔQ_i, $P = 0.29$), so we opted to use the full Bogus Creek dataset and exclude those two covariates from the model selection process.

For the Scott River, the model with the lowest AIC included photoperiod, mainstem discharge in September, and weekly change in discharge (Table 23). The model with the next lowest AIC, which differed by its inclusion of weekly temperature and an interaction between photoperiod and temperature, was also well supported ($P_R = 0.78$). For the Shasta River, the model with the lowest AIC included photoperiod, weekly temperature, weekly discharge, and an interaction between photoperiod and weekly temperature (Table 24). There was substantial support for the model with the next lowest AIC ($P_R = 0.92$), which differed by its inclusion of change in discharge. For Bogus Creek, the migration model with the lowest AIC included photoperiod, weekly temperature, and an interaction between those covariates (Table 25). There was modest support for the model with the next lowest AIC ($P_R = 0.54$), which differed by its inclusion of mainstem temperature in September. The signs of each covariate were generally consistent among models. As expected, there was a significant, positive effect of photoperiod on stream entry probability in each tributary. In each model, the effect of weekly temperature was positive and its interaction with photoperiod was negative, indicating that warm tributary temperatures favor stream entry and that the magnitude of this effect is more pronounced later in the season. The effects of weekly discharge and change in discharge were positive in the Scott and Shasta Rivers, suggesting that elevated discharge and rapidly increasing discharge both favor stream entry. There was a significant, positive effect of mainstem discharge during September in the Scott River, indicating that elevated discharge near the mouth of the Klamath River favors earlier freshwater entry and, by extension, earlier stream entry.

We selected the most parsimonious model from each river and tested its ability to predict adult migration timing. Bar plots of observed and model-predicted weekly abundances demonstrated that the models generally captured the overall pattern of the spawning migration into each tributary (Figures 8-10).

Table 23. Coefficients and standard errors (parentheses) of fixed effects terms from generalized linear mixed models of adult migration timing in the Scott River. Models are sorted according to their relative probability (P_R) of being the most parsimonious. Covariates are defined as follows: P_i, weekly photoperiod; T_i, weekly temperature; T, temperature near mouth of Klamath River prior to migration period; Q_i maximum weekly discharge; ΔQ_i weekly change in discharge.

AIC	P_R	P_i	T_i	T	Q_i	Q	ΔQ_i	P_i x T_i	P_i x Q_i	P_i x ΔQ_i
383.02	--	-3.68 (0.41)				1.00 (0.27)	4.35 (0.58)			
383.51	0.78	-3.78 (0.40)	0.49 (0.32)			0.94 (0.26)	3.66 (0.64)	-0.36 (0.45)		
384.77	0.42	-3.74 (0.43)			0.20 (0.39)	0.92 (0.31)	4.21 (0.64)			
385.04	0.36	-3.86 (0.43)	0.53 (0.32)		0.26 (0.37)	0.83 (0.30)	3.45 (0.69)	-0.33 (0.46)		
390.94	0.02	-3.98 (0.46)	0.57 (0.34)		0.83 (0.35)		3.06 (0.71)	-0.47 (0.49)		
391.26	0.02	-3.83 (0.47)			0.85 (0.37)		3.87 (0.67)			
394.30	< 0.01	-4.40 (0.38)					4.25 (0.65)			-1.43 (0.91)
394.65	< 0.01	-3.69 (0.43)	0.44 (0.35)				3.72 (0.70)	-0.68 (0.48)		
394.78	< 0.01	-4.47 (0.39)					-3.52 (0.43)			
404.00	< 0.01	-4.93 (0.54)	1.22 (0.38)		1.15 (0.45)	0.62 (0.37)		-0.89 (0.56)		
404.86	< 0.01	-4.91 (0.55)	1.19 (0.38)		1.51 (0.41)			-0.93 (0.57)		
408.67	< 0.01	-4.77 (0.54)	1.22 (0.40)			1.10 (0.36)		-1.29 (0.56)		
415.32	< 0.01	-5.05 (0.62)			1.59 (0.52)	0.67 (0.45)				
415.56	< 0.01	-5.02 (0.62)			1.98 (0.47)					
416.59	< 0.01	-4.65 (0.55)	1.20 (0.41)					-1.60 (0.57)		
416.91	< 0.01	-4.98 (0.61)			2.00 (0.47)				-0.45 (0.56)	
422.61	< 0.01	-4.81 (0.62)				1.42 (0.44)				
423.09	< 0.01	-4.65 (0.57)	1.47 (0.43)							
431.70	< 0.01	-4.57 (0.62)								
432.29	< 0.01	-4.63 (0.62)		-0.53 (0.44)						

Table 24. Coefficients and standard errors (parentheses) of fixed effects terms from generalized linear mixed models of adult migration timing in the Shasta River. Models are sorted according to their relative probability (P_R) of being the most parsimonious. Covariates are defined as follows: P_i, weekly photoperiod; T_i, weekly temperature; T, temperature near mouth of Klamath River prior to migration period; Q_i maximum weekly discharge; ΔQ_i weekly change in discharge.

AIC	P_R	P_i	T_i	T	Q_i	Q	ΔQ_i	P_i x T_i	P_i x Q_i	P_i x ΔQ_i
592.02	--	-2.31 (0.21)	0.44 (0.16)		0.49 (0.17)			-0.40 (0.25)		
592.18	0.92	-2.22 (0.22)	0.41 (0.16)		0.45 (0.17)		0.70 (0.51)	-0.35 (0.25)		
597.09	0.08	-2.11 (0.22)	0.29 (0.16)				0.92 (0.53)	-0.55 (0.24)		
598.19	0.05	-2.23 (0.22)	0.32 (0.16)					-0.65 (0.24)		
598.84	0.03	-2.12 (0.22)	0.30 (0.16)			0.08 (0.15)	0.90 (0.53)	-0.55 (0.24)		
599.02	0.03	-2.09 (0.23)	0.30 (0.16)	0.04 (0.16)			0.96 (0.54)	-0.56 (0.25)		
599.75	0.02	-2.25 (0.22)	0.33 (0.16)			0.10 (0.16)		-0.64 (0.24)		
600.16	0.02	-2.23 (0.22)	0.32 (0.17)	-0.03 (0.16)				-0.64 (0.25)		
600.80	0.01	-2.11 (0.23)	0.30 (0.16)	0.04 (0.16)		0.07 (0.15)	-0.93 (0.55)	-0.56 (0.25)		
601.36	0.01	-2.31 (0.23)			0.50 (0.17)					
601.70	0.01	-2.25 (0.22)	0.32 (0.16)	-0.04 (0.16)		0.11 (0.16)		-0.63 (0.25)		
601.76	0.01	-2.28 (0.23)			0.49 (0.17)				-0.30 (0.24)	
602.95	< 0.01	-2.21 (0.23)	0.44 (0.17)							
603.16	< 0.01	-2.03 (0.23)					1.40 (0.54)			
604.79	< 0.01	-1.99 (0.24)					1.00 (0.85)			-0.57 (0.94)
605.01	< 0.01	-2.04 (0.24)				0.06 (0.16)	1.38 (0.54)			
605.03	< 0.01	-2.05 (0.24)		-0.07 (0.17)			1.34 (0.56)			
606.85	< 0.01	-2.07 (0.24)		-0.07 (0.17)		0.07 (0.16)	1.31 (0.57)			
607.90	< 0.01	-1.66 (0.17)								
608.67	< 0.01	-2.24 (0.23)		-0.18 (0.16)						
609.49	< 0.01	-2.22 (0.23)				0.11 (0.17)				
610.17	< 0.01	-2.26 (0.24)		-0.19 (0.16)		0.12 (0.17)				

Table 25. Coefficients and standard errors (parentheses) of fixed effects terms from generalized linear mixed models of adult migration timing in Bogus Creek. Models are sorted according to their relative probability (PR) of being the most parsimonious. Covariates are defined as follows: P_i, weekly photoperiod; T_i, weekly temperature; T, temperature near mouth of Klamath River prior to migration period; Q_i maximum weekly discharge; ΔQ_i weekly change in discharge.

AIC	P_R	P_i	T_i	T	Q	P_i x T_i
577.83	--	-3.46 (0.20)	0.28 (0.14)			-0.47 (0.21)
579.05	0.54	-3.46 (0.20)	0.29 (0.14)	-0.11 (0.13)		-0.45 (0.21)
579.52	0.43	-3.45 (0.20)	0.27 (0.14)		-0.06 (0.12)	-0.47 (0.21)
580.58	0.25	-3.44 (0.21)	0.40 (0.14)			
580.89	0.22	-3.45 (0.20)	0.28 (0.14)	-0.10 (0.13)	-0.05 (0.12)	-0.45 (0.21)
586.49	0.01	-3.45 (0.22)				
587.65	0.01	-3.46 (0.22)		-0.13 (0.14)		
588.13	0.01	-3.45 (0.22)			-0.08 (0.13)	
589.46	< 0.01	-3.45 (0.22)		-0.12 (0.14)	-0.06 (0.13)	

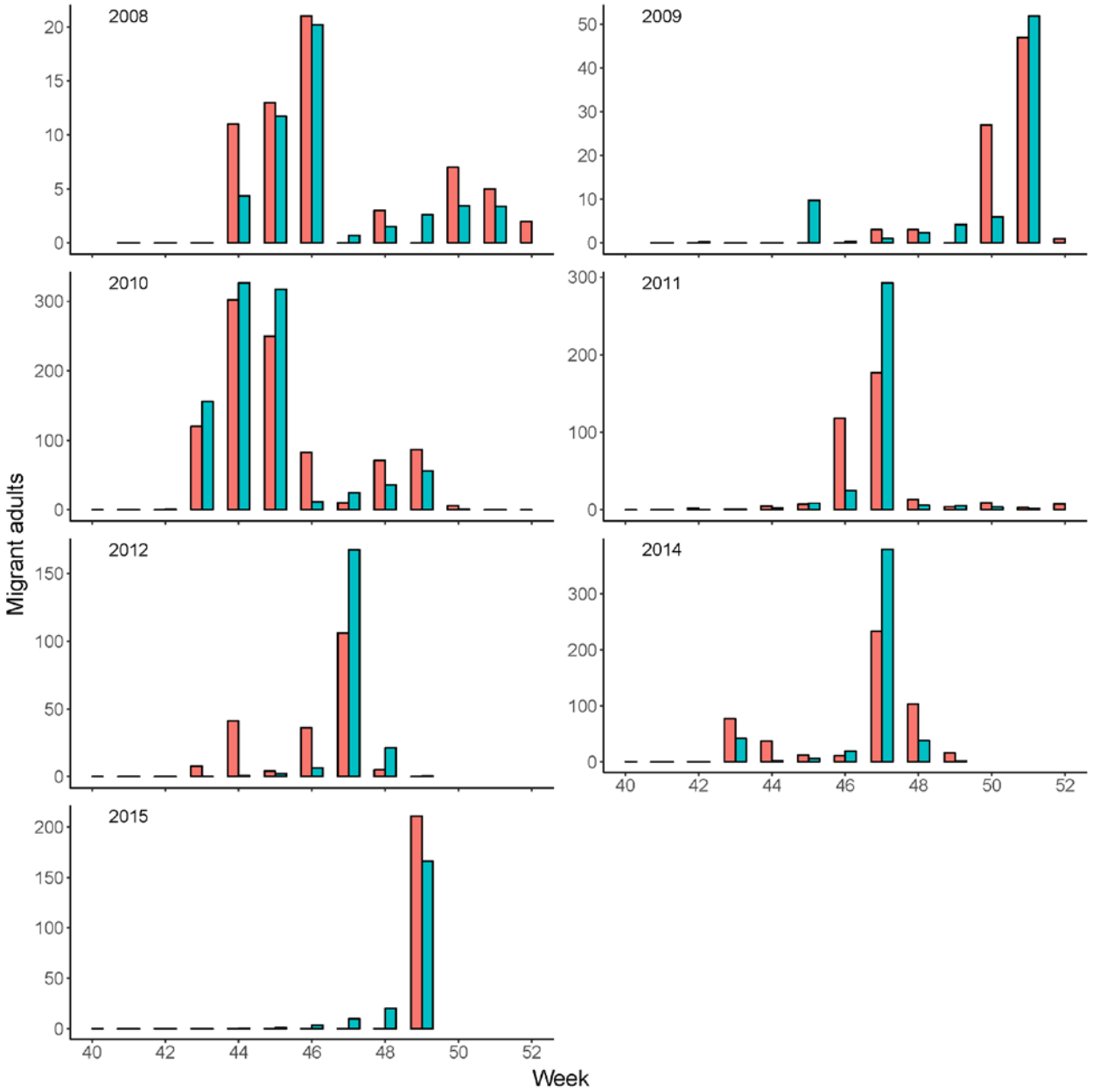

Figure 8. Weekly adult abundances predicted by the Scott River adult migration model (blue) and observed at the Scott River counting weir (red) during each spawning migration. Note that y-axis scales vary among years.

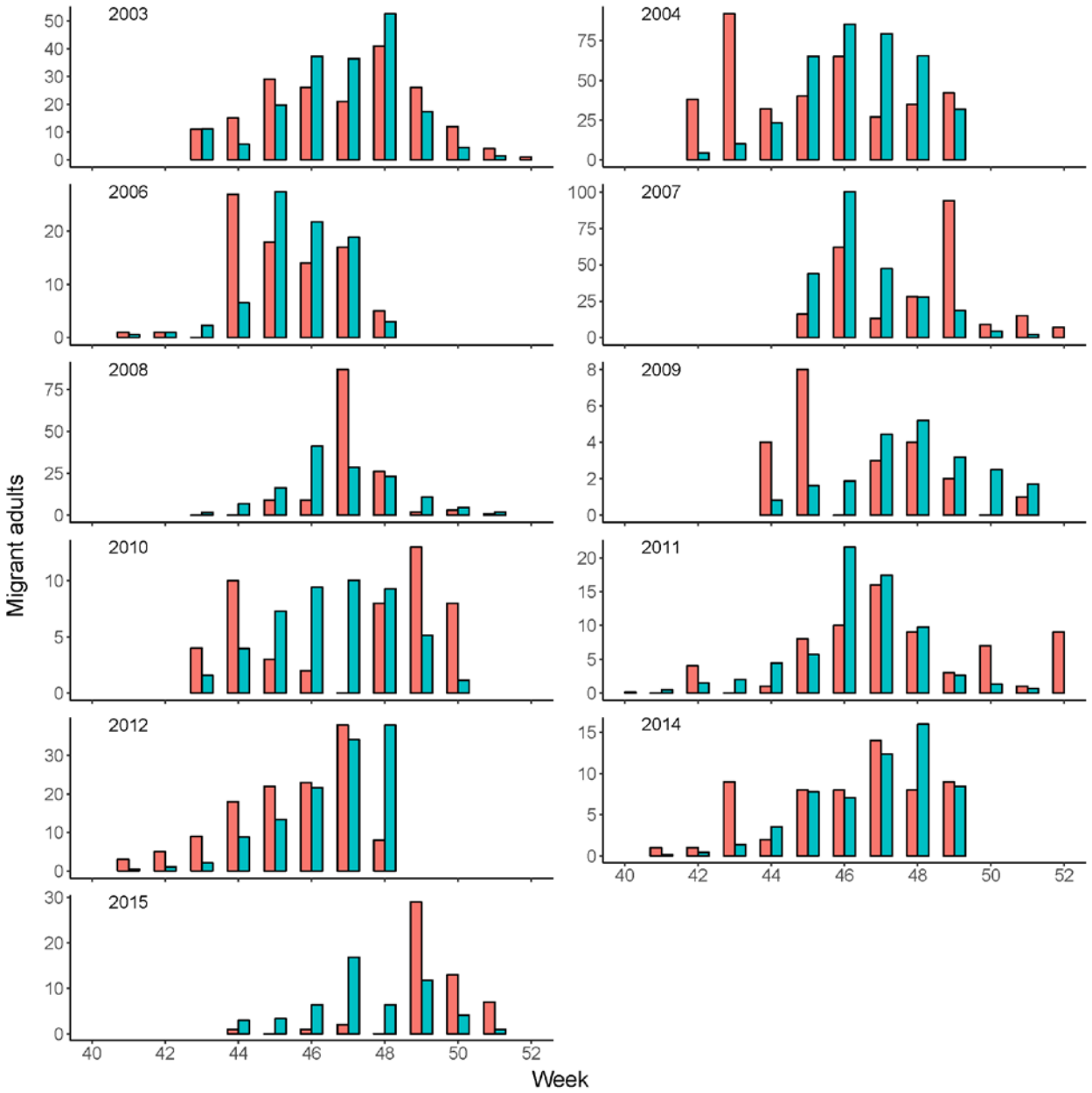

Figure 9. Weekly adult abundances predicted by the Shasta River adult migration model (blue) and observed at the Shasta River counting weir (red) during each spawning migration. Note that y-axis scales vary among years.

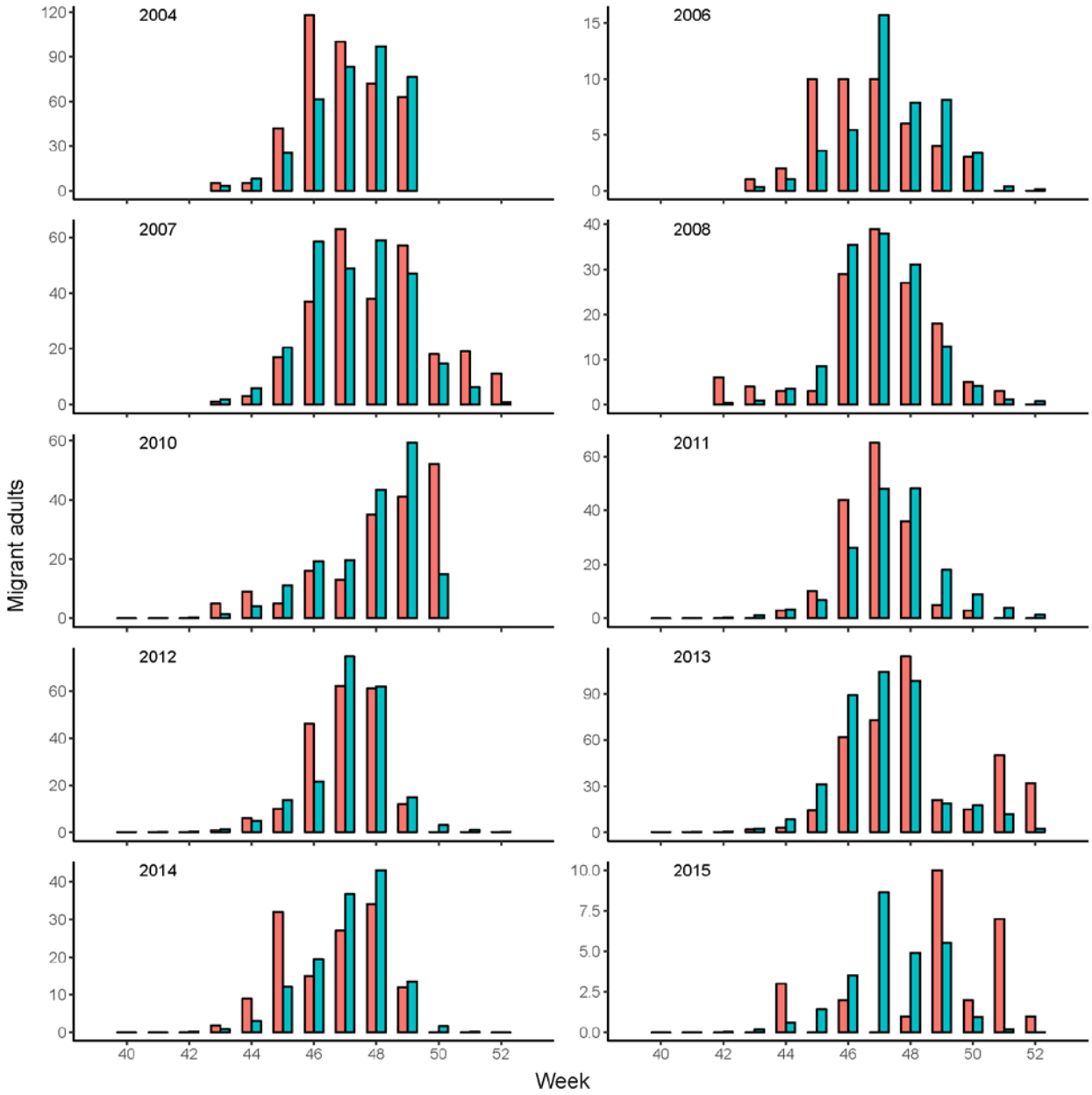

Figure 10. Weekly adult abundances predicted by the Bogus Creek adult migration model (blue) and observed at the Bogus Creek counting weir (red) during each spawning migration. Note that y-axis scales vary among years.

Emigration timing in the Scott and Shasta Rivers ·

We estimated generalized linear mixed models of parr emigration timing in the Scott and Shasta Rivers with most combinations of covariates and included interactions where there was a sufficient rationale for them. We assumed that accumulated temperature units (ATUs) was the primary factor governing migration timing of parr and that photoperiod was the primary factor governing migration timing of smolts.. We included ATUs in each parr emigration model and photoperiod in each smolt emigration model.

For the Scott River, the parr emigration model with the lowest AIC included ATUs, mean weekly stream temperature, maximum weekly decrease in stream flow, and an interaction between ATUs and change in stream flow (Table 26). As expected, emigration probability increased as ATUs increased. The combined effect of change in stream flow and its interaction with ATUs indicated that there is a tendency of parr to emigrate with decreasing flows and that this tendency is greatest in early spring. Although several of the best supported models included effects of mean weekly stream temperature and stream flow, the effects of these covariates were small and inconsistent with expectations. The smolt emigration model with the lowest AIC included photoperiod, pre-emigration temperature, weekly temperature, weekly discharge, ebb event, and an interaction between photoperiod and flood event (Table 27). Consistent with expectations, the effect of photoperiod on emigration probability was positive. The effects of both temperature indices were positive, indicating that warm temperatures favor emigration. The effect of weekly mean stream flow was negative, indicating that smolts tended to emigrate during periods of low stream flows. The combined effects of an ebb event and its interaction with photoperiod indicated that smolts tend to emigrate in weeks following rapid decreases in discharge and that this response is heightened earlier in the emigration period. Comparisons of this model with the other models produced little support for the model with the next lowest AIC (P_R = 0.02). Bar plots of mark-recapture estimated and model-predicted abundances of migrants demonstrated that the parr emigration model typically captured the migration pattern in late spring (Figure 11), but failed to capture large pulses of parr that emigrated in early spring in some years, most notably 2009 and 2010. The smolt emigration model was very effective at predicting the overall migration pattern (Figure 12). In particular, the model captured the tendency of smolts to emigrate early in the season following substantial declines in flow, as evidenced by the emigrations of 2009, 2014, and 2015.

Table 26. Coefficients and standard errors (parentheses) of fixed effects terms from generalized linear mixed models of parr emigration timing in the Scott River. Models are sorted according to their relative probability (P_R) of being the most parsimonious. Covariates are defined as follows: P_i, weekly photoperiod; T_i, weekly temperature; T, temperature near mouth of Klamath River prior to migration period; Q_i maximum weekly discharge; ΔQ_i weekly change in discharge.

AIC	P_R	ATU_i	Q_i	ΔQ_i	T_i	ΔT_i	ATU_i x Q_i	ATU_i x ΔQ_i	ATU_i x T_i	ATU_i x ΔT_i
808.30	--	3.92 (0.75)		-1.85 (0.56)	-1.62 (0.84)			-1.61 (0.48)		
809.17	0.65	4.08 (0.76)		-1.88 (0.56)	-1.77 (0.85)	0.31 (0.29)		-1.64 (0.47)		
809.37	0.59	2.72 (0.39)	0.69 (0.43)	-2.04 (0.67)				-1.71 (0.53)		
809.57	0.53	3.66 (0.80)	0.40 (0.48)	-2.16 (0.67)	-1.27 (0.94)			-1.80 (0.53)		
809.91	0.45	2.71 (0.40)		-1.33 (0.49)				-1.26 (0.44)		
810.54	0.33	3.84 (0.82)	0.38 (0.47)	-2.16 (0.67)	-1.44 (0.95)	0.30 (0.29)		-1.82 (0.53)		
811.41	0.21	2.75 (0.40)		-1.31 (0.49)		0.21 (0.30)		-1.26 (0.44)		
814.37	0.05	2.98 (0.40)	-0.27 (0.32)				-0.74 (0.37)			
814.82	0.04	3.17 (0.39)								
816.21	0.02	3.09 (0.40)		-0.24 (0.30)						
816.27	0.02	3.20 (0.39)				0.23 (0.31)				
816.39	0.02	3.09 (0.40)	-0.22 (0.33)							
816.43	0.02	3.67 (0.81)			-0.47 (0.80)				0.75 (0.49)	
816.78	0.01	3.31 (0.78)			-0.17 (0.78)					
817.74	0.01	3.71 (0.87)	-0.43 (0.42)		-0.81 (0.99)					
817.89	0.01	3.13 (0.41)	-0.20 (0.33)			0.22 (0.31)				
818.08	0.01	3.17 (0.40)				0.21 (0.32)				-0.15 (0.35)
818.15	0.01	3.44 (0.80)			-0.28 (0.79)	0.25 (0.32)				
818.99	0.01	3.87 (0.88)	-0.45 (0.42)		-0.96 (1.01)	0.27 (0.31)				

Table 27. Coefficients and standard errors (parentheses) of fixed effects terms from generalized linear mixed models of smolt emigration timing in the Scott River. Models are sorted according to their relative probability (P_R) of being the most parsimonious. Covariates are defined as follows: P_i, weekly photoperiod; T_i, weekly temperature; T, temperature near mouth of Klamath River prior to migration period; Q_i maximum weekly discharge; ΔQ_i weekly change in discharge.

AIC	P_R	P_i	T_i	T	Q_i	E_i	P_i x T_i	P_i x Q_i	P_i x E_i
2547.75	--	1.71 (0.21)	0.83 (0.23)	0.32 (0.10)	-0.69 (0.11)	1.14 (0.27)			-1.40 (0.28)
2555.75	0.02	1.66 (0.22)	0.90 (0.23)		-0.61 (0.11)	1.12 (0.28)			-1.46 (0.29)
2558.74	< 0.01	2.37 (0.12)		0.36 (0.10)	-0.78 (0.11)	1.11 (0.28)			-1.59 (0.29)
2568.23	< 0.01	2.38 (0.12)			-0.71 (0.11)	1.08 (0.29)			-1.68 (0.29)
2581.82	< 0.01	1.36 (0.23)	1.20 (0.25)			0.70 (0.29)			-1.57 (0.31)
2589.60	< 0.01	1.31 (0.23)	1.06 (0.26)	0.36 (0.12)	-0.58 (0.12)				
2596.87	< 0.01	1.23 (0.23)	1.15 (0.26)		-0.51 (0.12)				
2601.11	< 0.01	2.30 (0.13)		0.22 (0.12)		0.52 (0.30)			-1.87 (0.32)
2602.75	< 0.01	2.31 (0.13)				0.54 (0.31)			-1.91 (0.32)
2604.03	< 0.01	2.12 (0.12)		0.41 (0.12)	-0.72 (0.12)				
2608.85	< 0.01	0.97 (0.23)	1.40 (0.26)	0.25 (0.12)					
2610.99	< 0.01	0.95 (0.23)	1.43 (0.27)						
2612.07	< 0.01	1.11 (0.29)	1.28 (0.31)				0.20 (0.21)		
2613.27	< 0.01	2.11 (0.13)			-0.65 (0.12)				
2613.53	< 0.01	2.09 (0.13)			-0.60 (0.13)			-0.19 (0.15)	
2632.44	< 0.01	2.01 (0.13)				0.84 (0.33)			
2633.87	< 0.01	2.02 (0.13)		0.28 (0.13)					
2636.61	< 0.01	2.01 (0.13)							

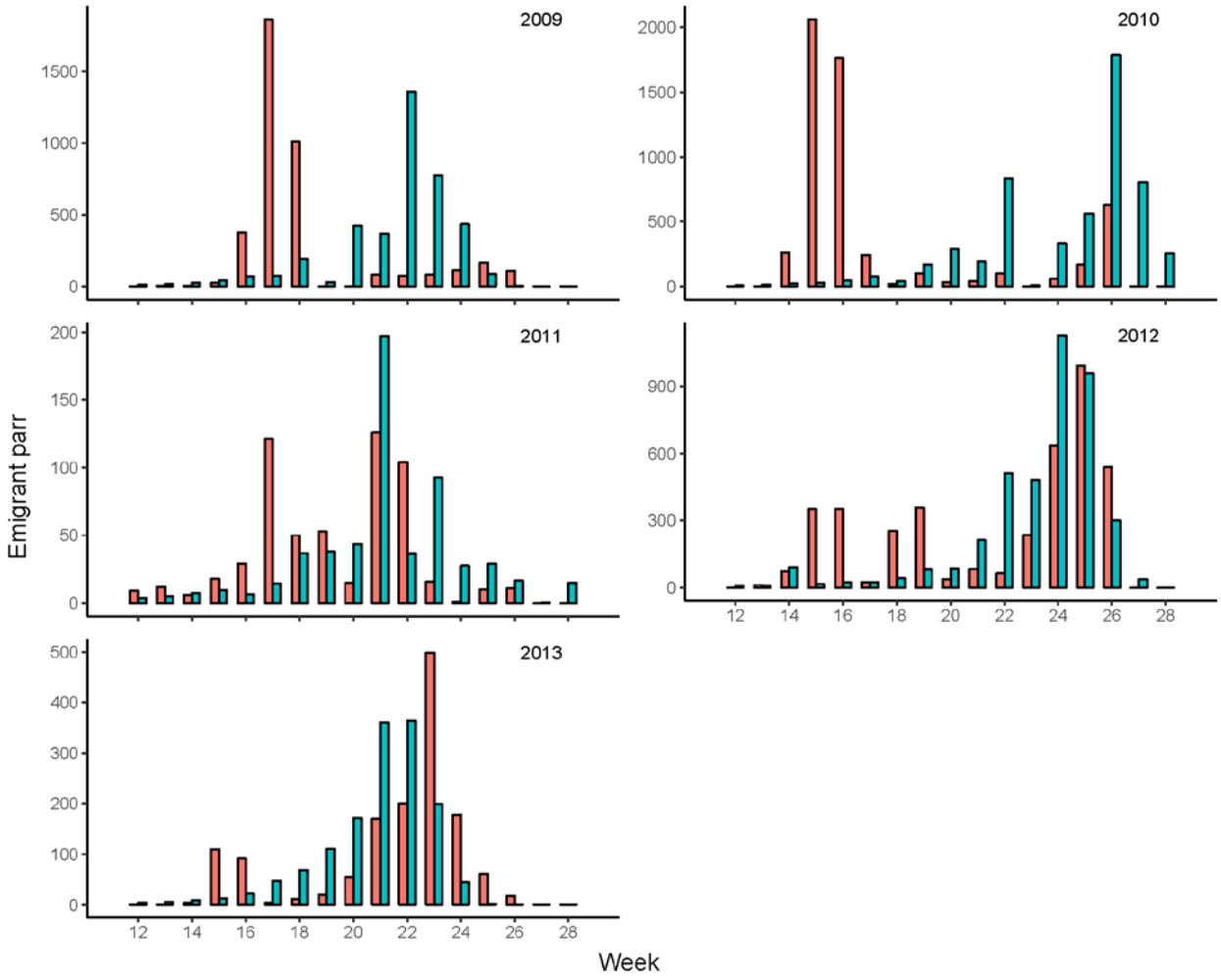

Figure 11. Weekly parr abundances predicted by the Scott River emigration model (blue) and estimated by mark-recapture studies (red) during each emigration period. Note that y-axis scales vary among years.

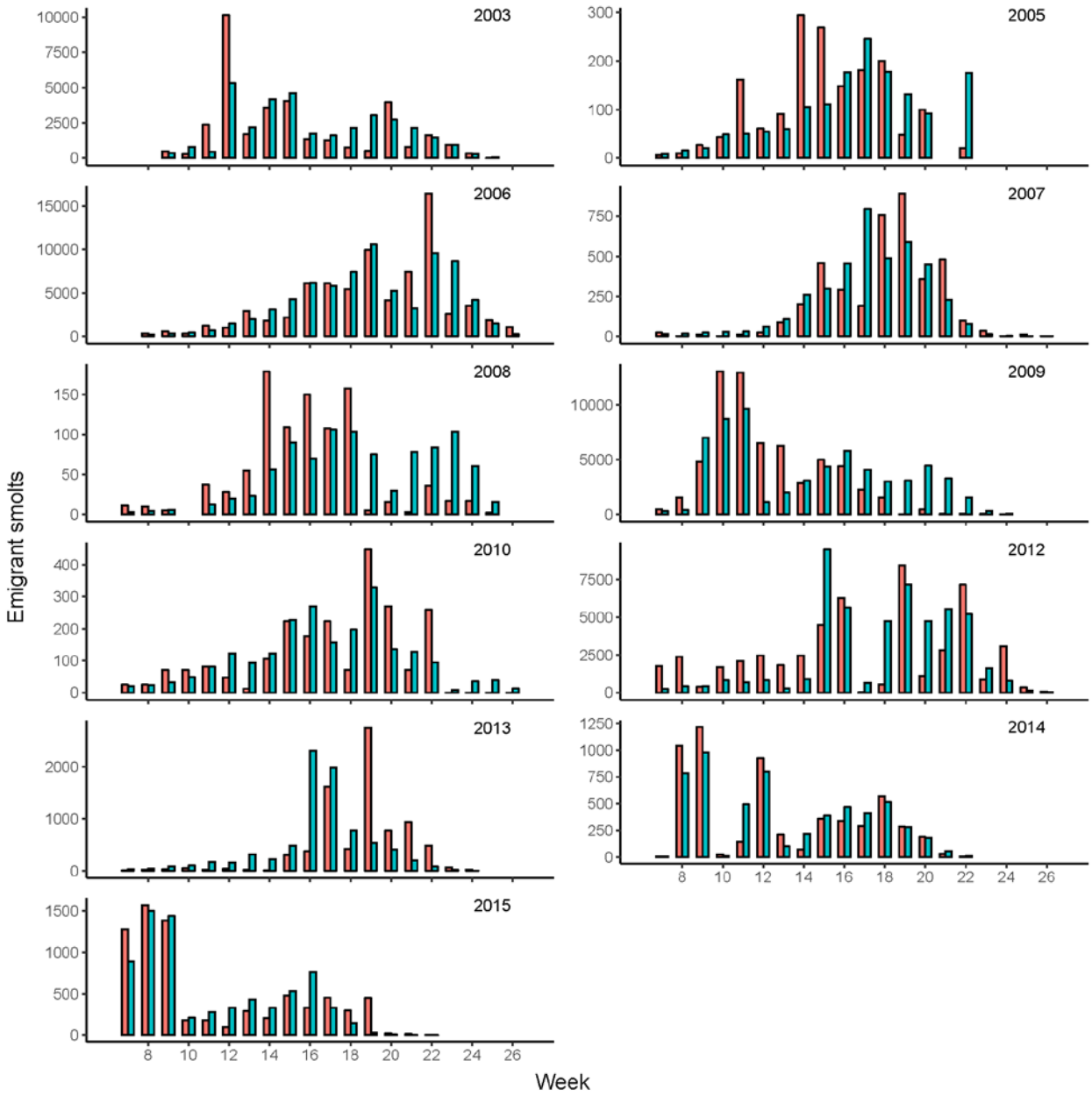

Figure 12. Weekly smolt abundances predicted by the Scott River emigration model (blue) and estimated by mark-recapture studies (red) during each emigration period. Note that y-axis scales vary among years.

For the Shasta River, the parr emigration model with the lowest AIC included ATUs, mean weekly stream temperature, and an interaction between ATUs and stream temperature (Table 28). As was observed in the Scott River, emigration probability increased as ATUs increased. The combined effect of stream temperature and its interactions with ATUs indicated that parr tended to leave the Shasta River during warm weeks and that this effect was greatest in early spring. Another model that included a positive effect of maximum weekly increase in temperature was also well supported (P_R = 0.71), but the standard error of the effect was large. The smolt emigration model with lowest AIC included photoperiod,

pre-emigration temperature, weekly temperature, irrigation event, and an interaction between photoperiod and irrigation event (Table 29). The effects of photoperiod and the two temperature indices were positive, as was observed in the Scott River model. The combined effect of irrigation and its interaction with photoperiod indicated that smolt emigration probability increased dramatically following the reduction in flow that accompanies the start of irrigation season and that the response to the reduction in flow was greatest early in the emigration period. There was minimal support for the model with the next lowest AIC (P_R = 0.37). Bar plots of mark-recapture estimated and model-predicted abundances of smolts demonstrated that the parr emigration model was generally effective at predicting the overall migration pattern, including pulses of fish that appeared to emigrate in response to high stream temperatures (Figure 13). A notable exception to this was 2013, in which the model failed to capture a large pulse of emigrant parr in early spring. The smolt emigration model predicted the overall migration pattern effectively in most years (Figure 14), but spuriously predicted a late migration in 2003 when the model failed to capture an early pulse of fish.

Summer refuge entry timing in small tributaries ·

We estimated generalized linear mixed models of thermal refuge entry timing in summer with most combinations of covariates (Table 30). There were several covariates that were highly correlated and were therefore not modeled together. The most parsimonious model of refuge entry timing included temperature in the mainstem. The positive effect of this covariate indicates that redistributing parr have a tendency to enter thermal refugia as the mainstem undergoes seasonal warming. The model with the next lowest AIC score, which differed by its inclusion of change in discharge (PR = 0.70), was also well supported. We used the most parsimonious model of thermal refuge entry timing to predict weekly frequencies of immigrant parr and compared those estimates to frequencies of parr observed at fyke nets and stationary PIT arrays in each refuge. Bar plots revealed that the predicted frequency distributions typically overlapped the observed frequency distributions (Figure 15), thereby demonstrating that our model captured the primary characteristics of refuge entry timing in most years. A notable exception was the migration into Waukell Creek in 2010, when two early pulses of parr were triggered by unknown factors. Consequently, the model underestimated the number of parr entering the refuge early in the redistribution period and overestimated later in the period.

Table 28. Coefficients and standard errors (parentheses) of fixed effects terms from generalized linear mixed models of parr emigration timing in the Shasta River. Models are sorted according to their relative probability (P_R) of being the most parsimonious. Covariates are defined as follows: ATU_i, accumulated temperature units; Q_i, weekly discharge; ΔQ_i, weekly change in discharge; T_i, weekly temperature; ΔT_i, weekly change in temperature

AIC	P_R	ATU_i	Q_i	ΔQ_i	T_i	ΔT_i	ATU_i x Q_i	ATU_i x ΔQ_i	ATU_i x T_i	ATU_i x ΔT_i
1382.07	--	1.08 (0.42)			2.29 (0.42)				0.47 (0.24)	
1382.75	0.71	1.19 (0.43)			2.16 (0.43)	0.25 (0.22)			0.51 (0.25)	
1383.84	0.41	1.27 (0.42)			2.16 (0.42)					
1384.07	0.37	1.08 (0.42)		-0.01 (0.23)	2.29 (0.42)				0.48 (0.25)	
1384.73	0.26	1.19 (0.43)		-0.03 (0.23)	2.15 (0.44)	0.25 (0.22)			0.52 (0.25)	
1386.00	0.14	1.08 (0.43)	-0.07 (0.38)		2.26 (0.44)		-0.09 (0.33)		0.42 (0.34)	
1387.99	0.05	1.08 (0.43)	-0.06 (0.43)	-0.03 (0.31)	2.26 (0.44)		-0.10 (0.34)		0.41 (0.35)	
1388.70	0.04	1.19 (0.44)	-0.03 (0.43)	-0.05 (0.31)	2.13 (0.46)	0.25 (0.22)	-0.06 (0.34)		0.48 (0.35)	
1402.79	< 0.01	2.83 (0.32)	-0.69 (0.38)	0.51 (0.23)			-0.53 (0.27)			
1402.79	< 0.01	2.83 (0.32)	-0.69 (0.38)			0.51 (0.23)	-0.52 (0.27)			
1402.84	< 0.01	3.19 (0.24)				0.53 (0.24)				
1403.61	< 0.01	3.18 (0.24)				0.49 (0.24)				-0.29 (0.26)
1404.50	< 0.01	3.16 (0.25)		-0.15 (0.25)		0.54 (0.24)				
1404.67	< 0.01	2.86 (0.33)	-0.61 (0.46)	-0.12 (0.34)		0.52 (0.23)	-0.54 (0.28)			
1405.68	< 0.01	2.81 (0.32)	-0.75 (0.39)				-0.53 (0.28)			
1406.00	< 0.01	3.21 (0.25)								
1407.26	< 0.01	3.06 (0.30)	-0.25 (0.29)							
1407.70	< 0.01	3.18 (0.25)		-0.14 (0.25)						
1409.48	< 0.01	3.17 (0.25)		-0.24 (0.33)				-0.12 (0.26)		

Table 29. Coefficients and standard errors (parentheses) of fixed effects terms from generalized linear mixed models of smolt emigration timing in the Shasta River. Models are sorted according to their relative probability (P_R) of being the most parsimonious. Covariates are defined as follows: P_i, weekly photoperiod; T_i, weekly temperature; T, temperature near mouth of Klamath River prior to migration period; Q_i maximum weekly discharge; ΔQ_i weekly change in discharge.

AIC	P_R	P_i	T_i	T	Q_i	I_i	P_i x Q_i	P_i x I_i
1501.52	--	2.18 (0.41)	1.56 (0.34)	0.43 (0.14)		1.37 (0.37)		-2.54 (0.44)
1503.49	0.37	2.19 (0.41)	1.54 (0.37)	0.44 (0.14)	-0.04 (0.20)	1.34 (0.42)		-2.54 (0.44)
1509.41	0.02	2.44 (0.41)	1.49 (0.35)			0.98 (0.36)		-2.70 (0.44)
1518.26	< 0.01	3.45 (0.31)		0.48 (0.15)	-0.34 (0.20)	1.17 (0.44)		-2.46 (0.47)
1519.11	< 0.01	3.54 (0.31)		0.40 (0.15)		1.51 (0.40)		-2.50 (0.47)
1526.06	< 0.01	3.70 (0.30)			-0.14 (0.19)	0.97 (0.45)		-2.65 (0.47)
1540.42	< 0.01	1.77 (0.41)	1.37 (0.44)	0.51 (0.17)	-0.46 (0.21)			
1543.09	< 0.01	1.78 (0.42)	1.71 (0.42)	0.36 (0.16)				
1546.41	< 0.01	1.84 (0.43)	1.61 (0.42)					
1547.48	< 0.01	1.85 (0.42)	1.46 (0.45)		-0.19 (0.20)			
1548.08	< 0.01	2.86 (0.24)		0.55 (0.17)	-0.70 (0.21)			
1554.99	< 0.01	3.07 (0.24)			-0.16 (0.24)		0.44 (0.25)	
1555.99	< 0.01	3.02 (0.24)			-0.42 (0.19)			
1557.21	< 0.01	3.34 (0.20)		0.31 (0.16)				
1558.75	< 0.01	3.32 (0.20)						

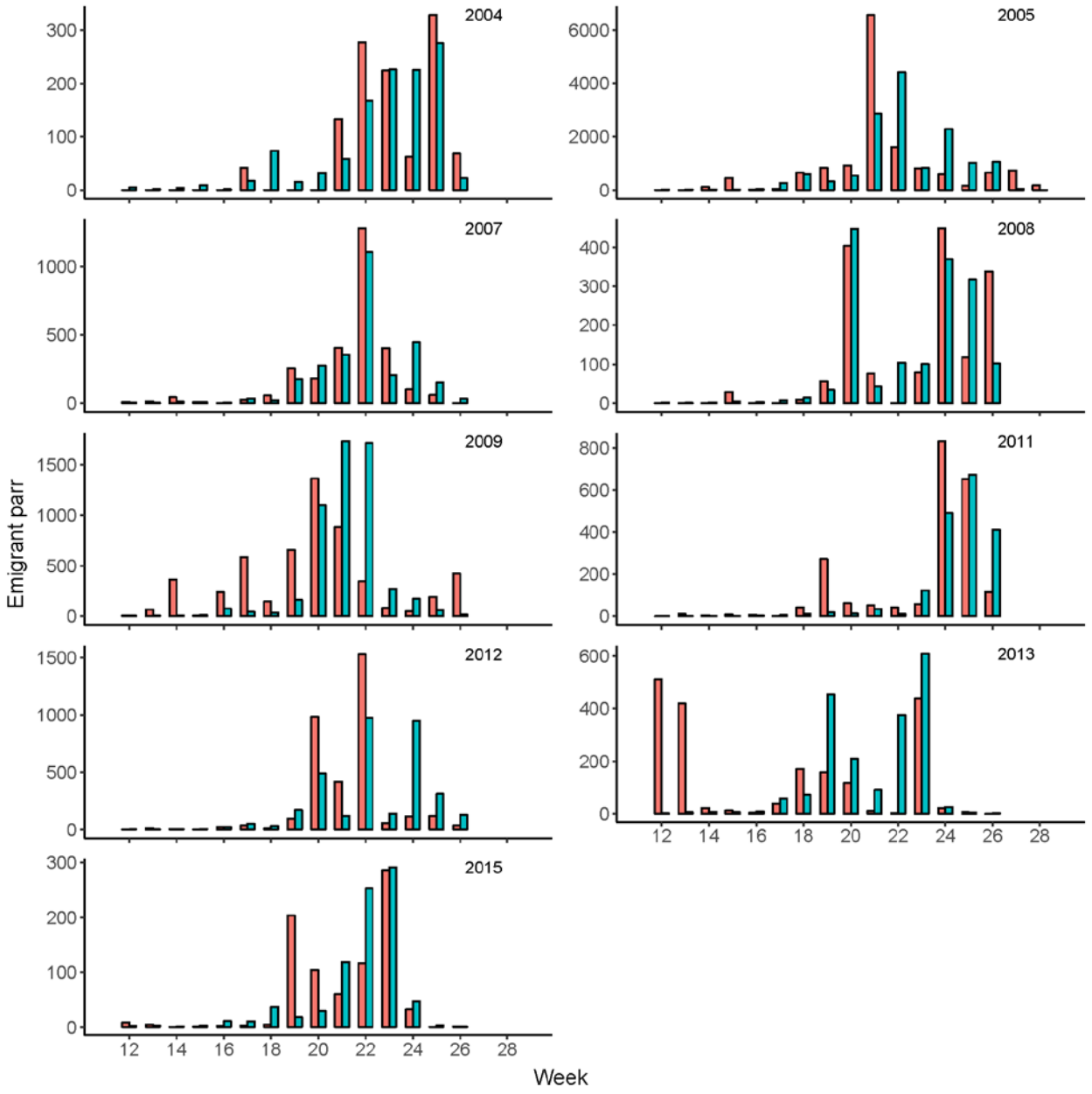

Figure 13. Weekly parr abundances predicted by the Shasta River emigration model (blue) and estimated by mark-recapture studies (red) during each emigration period. Note that y-axis scales vary among years.

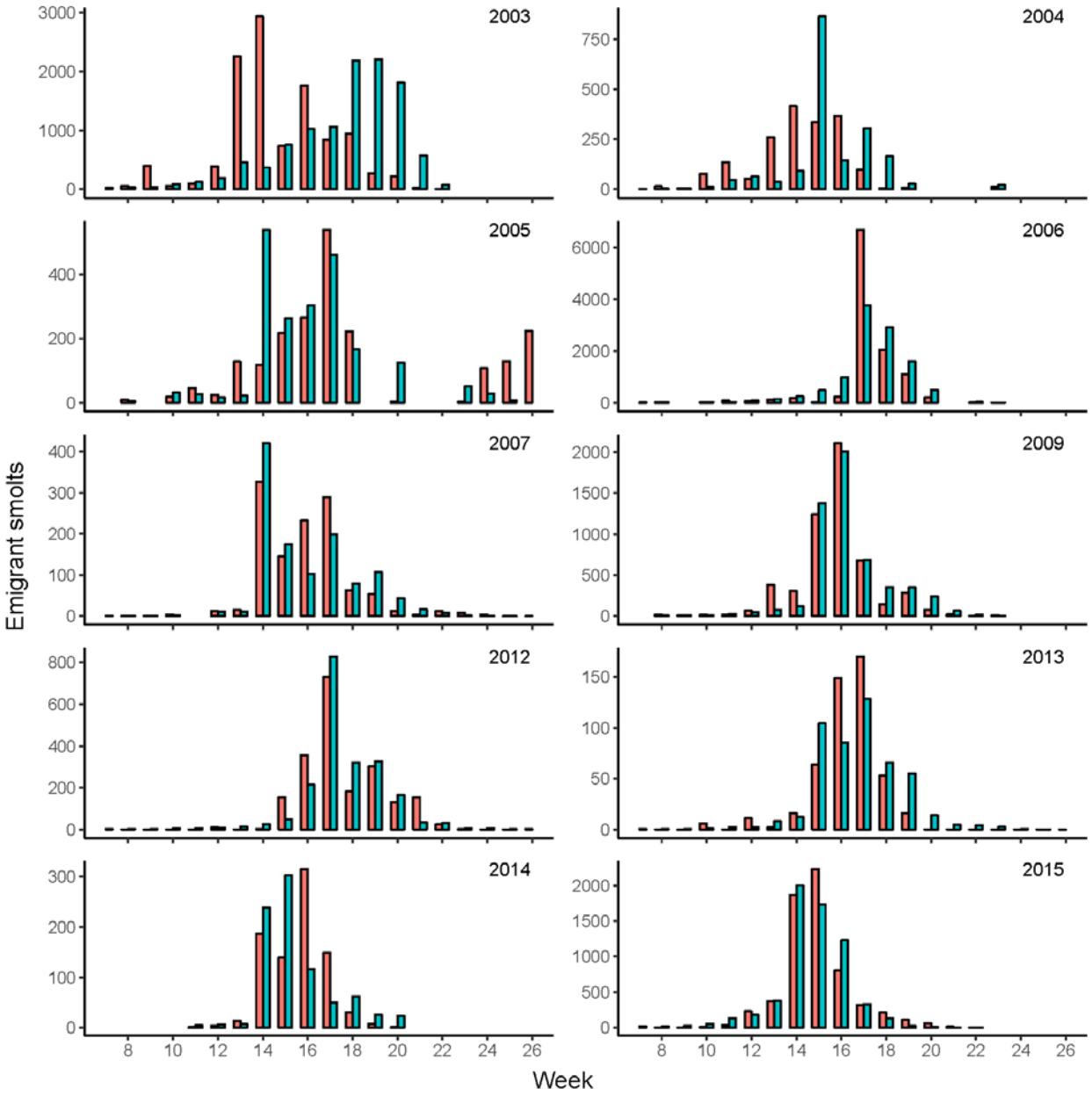

Figure 14. Weekly smolt abundances predicted by the Shasta River emigration model (blue) and estimated by mark-recapture studies (red) during each emigration period. Note that y-axis scales vary among years.

Winter emigration timing in small tributaries ·

Because we found minimal evidence of collinearity, we estimated generalized linear mixed models of winter emigration timing with all possible combinations of covariates (Table 31). The most parsimonious model of winter emigration probability included interval, weekly discharge, and flood event. The positive effect of weekly discharge indicated that parr tended to emigrate from rearing habitats during periods of elevated discharge. The positive effect of flood event and its negative interaction with interval indicated that parr tended to emigrate during periods of rapidly increasing discharge and that the magnitude of this effect is larger earlier in the winter emigration period. The model with the next lowest AIC score, which differed by its exclusion of weekly discharge, was moderately supported (PR = 0.71). We used the most parsimonious model of winter emigration timing to predict weekly frequencies of emigrant parr and compared those estimates to frequencies of parr observed at stationary arrays at each rearing site. Bar plots revealed that the predicted frequency distributions matched the observed frequency distributions reasonably well in most years (Figure 16), indicating that our model generally captured the relationship between winter hydrological patterns and emigration timing. A notable exception was the emigration from the Sandy Bar floodplain channel in 2010. During that overwintering period, there were several substantial increases in discharge early in the overwintering period that failed to trigger pulses of emigrants. Consequently, the model overestimated the number of parr emigrating from Sandy Bar early in the overwintering period and underestimated later in the period.

Winter refuge entry timing in small tributaries ·

We found minimal evidence of collinearity and therefore constructed generalized linear mixed models of winter refuge entry timing with all possible combinations of covariates (Table 32). The most parsimonious model of refuge entry timing included interval, flood event, and an interaction between them. The positive effect of flood event and its negative interaction with interval indicates that redistributing parr tend to enter winter refugia in concert with discharge increases in the Klamath River and that the magnitude of this effect is most pronounced early in the redistribution period. The models with next two lowest AIC scores included a model that differed by its exclusion of the interaction term (PR = 0.45) and a model that differed by its inclusion of Q_i^* (PR = 0.44). We estimated weekly frequencies of winter immigrants with the most parsimonious model of refuge entry timing and compared those estimates to frequencies observed at the upstream fyke net and at the stationary PIT array on lower Waukell Creek (Figure 17). The model approximated the frequency distribution in most years and successfully predicted large pulses of immigrants, presumably cued by discharge increases, on several occasions. A notable departure between predicted and observed frequencies occurred in 2009 when the model successfully predicted a large pulse of immigrants during week 43, but failed to predict large pulses in the following two weeks. This pattern indicates that a discharge increase in week 43 may have influenced immigration probability over subsequent weeks. However, such a protracted effect of discharge increases was generally not evident.

Table 30. Coefficients and standard errors (parentheses) of fixed effects terms from generalized linear mixed models of summer refuge entry timing in small tributaries. Models are sorted according to their relative probability (PR) of being the most parsimonious. Covariates are defined as follows: T_i^*, weekly temperature of the mainstem; ΔT_i^*, weekly change in temperature of the mainstem; Q_i^*, weekly discharge of the mainstem.

AIC	P_R	T_i^*	ΔT_i^*	Q_i^*	ΔQ_i^*
458.90	1.00	1.99 (0.17)			
459.61	0.70	2.08 (0.19)			0.19 (0.17)
460.31	0.49	1.92 (0.21)	-0.14 (0.20)		
460.34	0.49	2.02 (0.19)	-0.19 (0.17)		0.23 (0.16)
488.20	< 0.01		-0.43 (0.20)	-2.45 (0.30)	0.82 (0.24)
490.92	< 0.01			-2.59 (0.30)	0.74 (0.24)
497.30	< 0.01		-0.35 (0.22)	-1.82 (0.26)	
497.90	< 0.01			-1.98 (0.24)	
533.06	< 0.01		-0.81 (0.29)		-0.52 (0.26)
534.75	< 0.01		-1.00 (0.28)		
539.07	< 0.01				-0.76 (0.26)

Table 31. Coefficients and standard errors (parentheses) of fixed effect terms from generalized linear mixed models of winter emigration timing in small tributaries. Models are sorted according to their relative probability (P_R) of being the most parsimonious. Covariates are defined as follows: I_i, weekly index; Q_i, weekly discharge; F_i, flood event.

AIC	P_R	I_i	Q_i	F_i	I_i x Q_i	I_i x F_i
350.25	--	1.49 (0.36)	0.47 (0.28)	0.77 (0.57)		-1.91 (0.58)
350.94	0.71	1.71 (0.35)		1.09 (0.56)		-1.87 (0.60)
357.87	0.02	1.11 (0.31)		1.44 (0.60)		
359.33	0.01	0.81 (0.35)	0.63 (0.32)			
361.32	< 0.01	0.81 (0.35)	0.63 (0.32)		-0.03 (0.35)	
362.37	< 0.01		0.95 (0.30)			
362.52	< 0.01		0.83 (0.31)	0.92 (0.67)		
367.32	< 0.01			1.46 (0.69)		

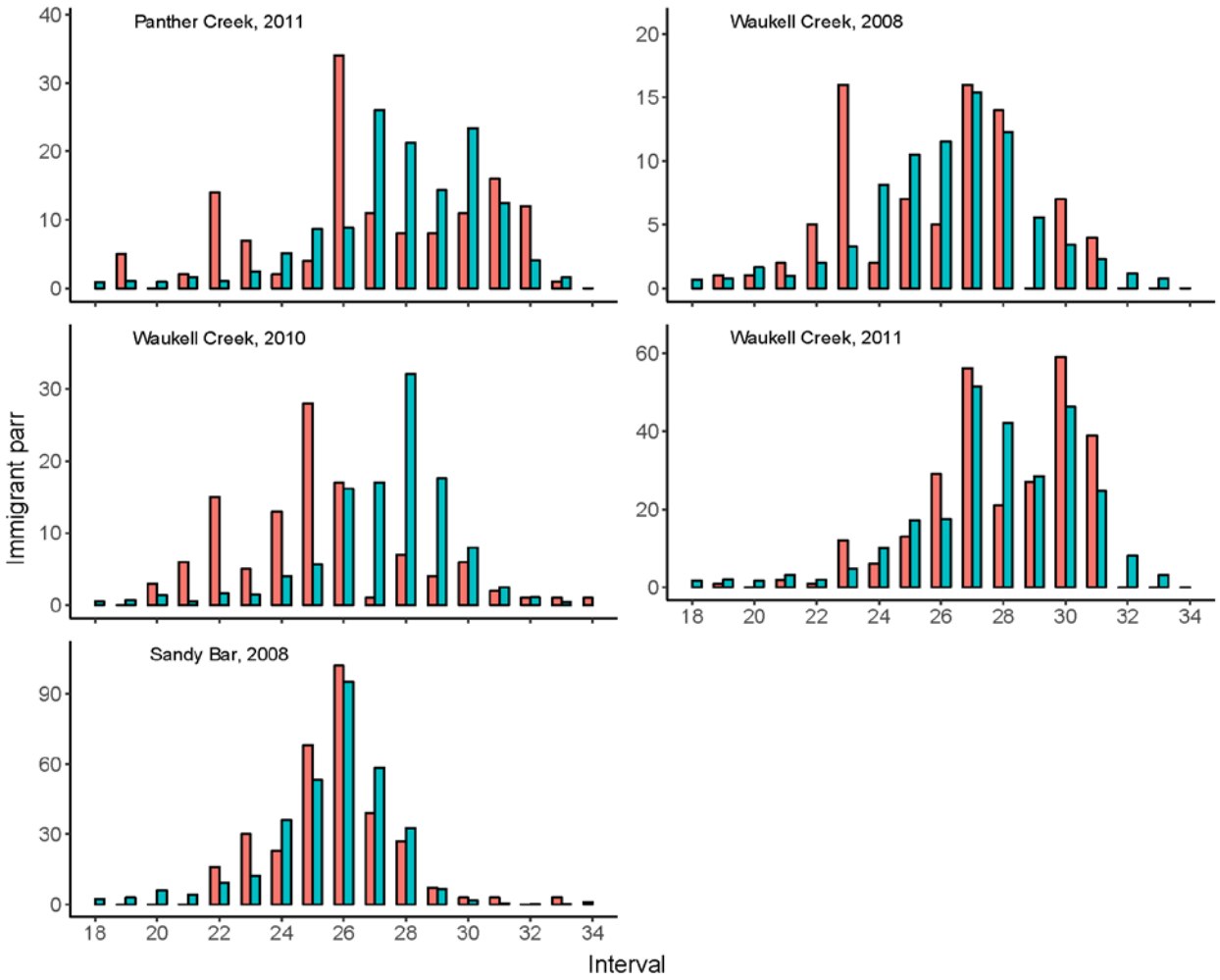

Figure 15. Frequencies of PIT-tagged parr entering thermal refuges during seven-day intervals as predicted by the model of summer refuge entry timing (blue) and as observed at monitoring sites (red). Monitoring was conducted by fyke nets and stationary PIT arrays in Panther Creek, Waukell Creek, and Sandy Bar floodplain channel. Note that y-axis scales vary among years.

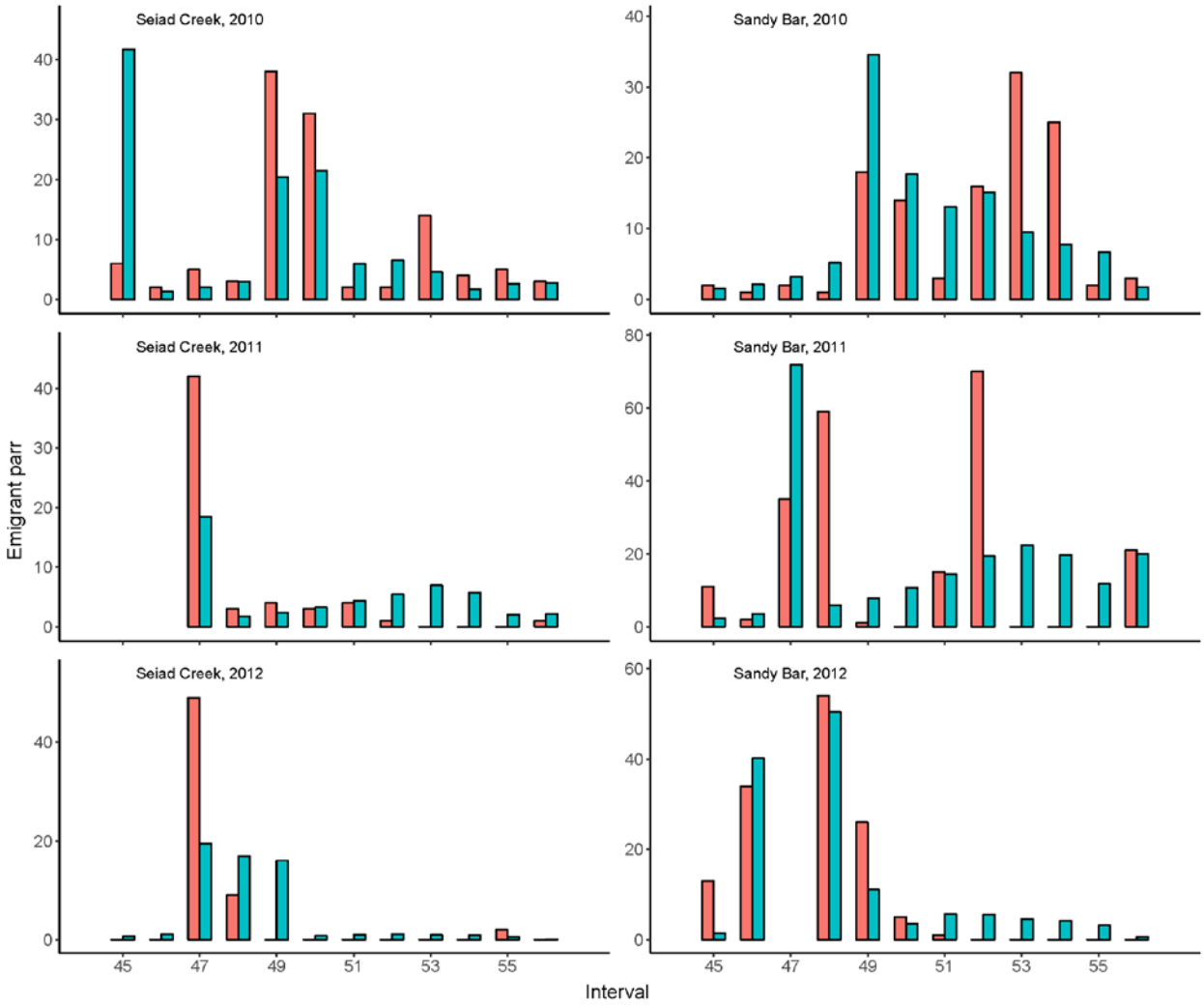

Figure 16. Frequencies of PIT-tagged parr emigrating from overwintering sites during seven-day intervals as predicted by the model of winter emigration timing (blue) and as observed at stationary PIT arrays (red). Monitoring was conducted in Sandy Bar floodplain channel and in Seiad Creek. Note that y-axis scales vary among years.

Smolt emigration timing in small tributaries ·

We estimated generalized linear mixed models of smolt emigration timing in Klamath River tributaries with most combinations of covariates, and we included interactions where there was a sufficient rationale to support them (Table 33). There were several covariates that were highly correlated and were therefore not modeled together. Because photoperiod was assumed to be the primary factor controlling smolt emigration timing, we included this covariate in each model. The most parsimonious model included photoperiod, tributary location, flood event, and an interaction between location and photoperiod. The positive effect of location and its interaction with photoperiod indicated that smolts have a tendency to emigrate earlier in the season in Middle Klamath Basin tributaries. The positive effect of flood event indicated that smolts have a tendency to emigrate following substantial

increases in discharge. The model with the next lowest AIC differed by its inclusion of weekly temperature and was moderately supported (PR = 0.52). Bar plots demonstrated that the model-predicted frequency distributions typically overlapped the observed frequency distributions (Figures 18, 19). In particular, the model captured large differences in migration timing between tributaries located in the lower and middle Klamath Basin. The model predicted a mean emigration date of 15 April for Seiad Creek, which was one month earlier than the mean emigration date predicted for the lower tributaries. There were several instances in which a large pulse of smolts was triggered by unknown factors, thereby causing the model to underestimate detection frequencies early in the emigration period and overestimate later in the period.

Table 32. Coefficients and standard errors (parentheses) of fixed effect terms from generalized linear mixed models of winter refuge entry timing in small tributaries. Models are sorted according to their relative probability (P_R) of being the most parsimonious. Covariates are defined as follows: I_i, weekly index; Q_i^*, weekly discharge in the mainstem; F_i^*, flood event in the mainstem.

AIC	P_R	I_i	Q_i^*	F_i^*	I_i x Q_i^*	I_i x F_i^*
643.94	--	0.37 (0.04)		2.52 (0.87)		-0.19 (0.10)
645.56	0.45	0.34 (0.04)		0.99 (0.38)		
645.58	0.44	0.34 (0.05)	0.88 (0.57)	2.05 (0.91)	-0.10 (0.07)	-0.14 (0.10)
648.70	0.09	0.30 (0.04)	1.35 (0.57)		-0.14 (0.07)	
650.10	0.05	0.35 (0.04)				
650.90	0.03	0.33 (0.04)	0.23 (0.20)			
693.75	< 0.01		0.86 (0.27)			
700.43	< 0.01			1.04 (0.58)		

Table 33. Coefficients and standard errors (parentheses) of fixed effects terms from generalized linear mixed models of smolt emigration timing in small tributaries. Models are sorted according to their relative probability (P_R) of being the most parsimonious. Covariates are defined as follows: P_i, photoperiod; K, location of tributary; T, temperature prior to the smolt emigration period; T_i, weekly temperature; F_i, flood event.

AIC	P_R	P_i	K	T	T_i	F_i	K x P_i	P_i x F_i
1487.09	--	2.47 (0.11)	1.28 (0.20)			0.47 (0.22)	-0.50 (0.21)	
1488.38	0.52	2.37 (0.16)	1.29 (0.20)		0.13 (0.15)	0.47 (0.22)	-0.49 (0.21)	
1489.53	0.30	2.44 (0.11)	1.22 (0.20)				-0.50 (0.21)	
1490.42	0.19	2.44 (0.11)	1.52 (0.34)	0.16 (0.15)			-0.51 (0.21)	
1490.89	0.15	2.35 (0.16)	1.22 (0.20)		0.12 (0.15)		-0.49 (0.21)	
1492.85	0.06	2.33 (0.10)	1.35 (0.19)					
1499.87	< 0.01	2.35 (0.10)				0.44 (0.22)		
1500.83	< 0.01	2.23 (0.15)			0.15 (0.15)	0.45 (0.22)		
1501.72	< 0.01	2.33 (0.10)				0.48 (0.24)		0.10 (0.26)
1501.79	< 0.01	2.32 (0.10)						
1501.87	< 0.01	2.35 (0.10)		0.01 (0.16)		0.44 (0.22)		
1504.62	< 0.01	2.18 (0.16)		0.08 (0.18)	0.18 (0.17)			

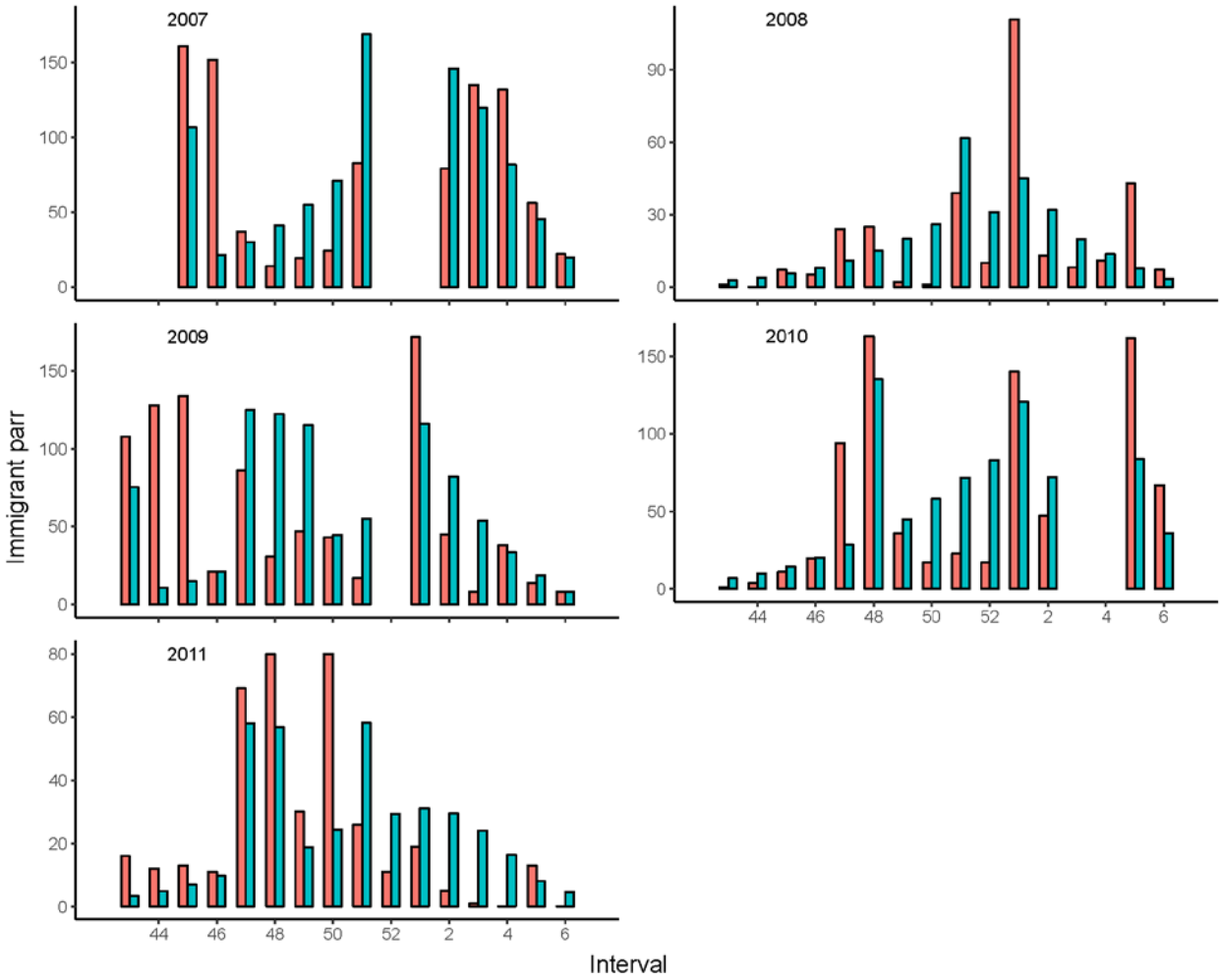

Figure 17. Frequencies of PIT-tagged parr immigrating into a winter refuge during seven-day intervals as predicted by the model of winter refuge entry timing (blue) and as observed at stationary PIT arrays (red). Monitoring was conducted at Waukell Creek. Note that y-axis scales vary among years.

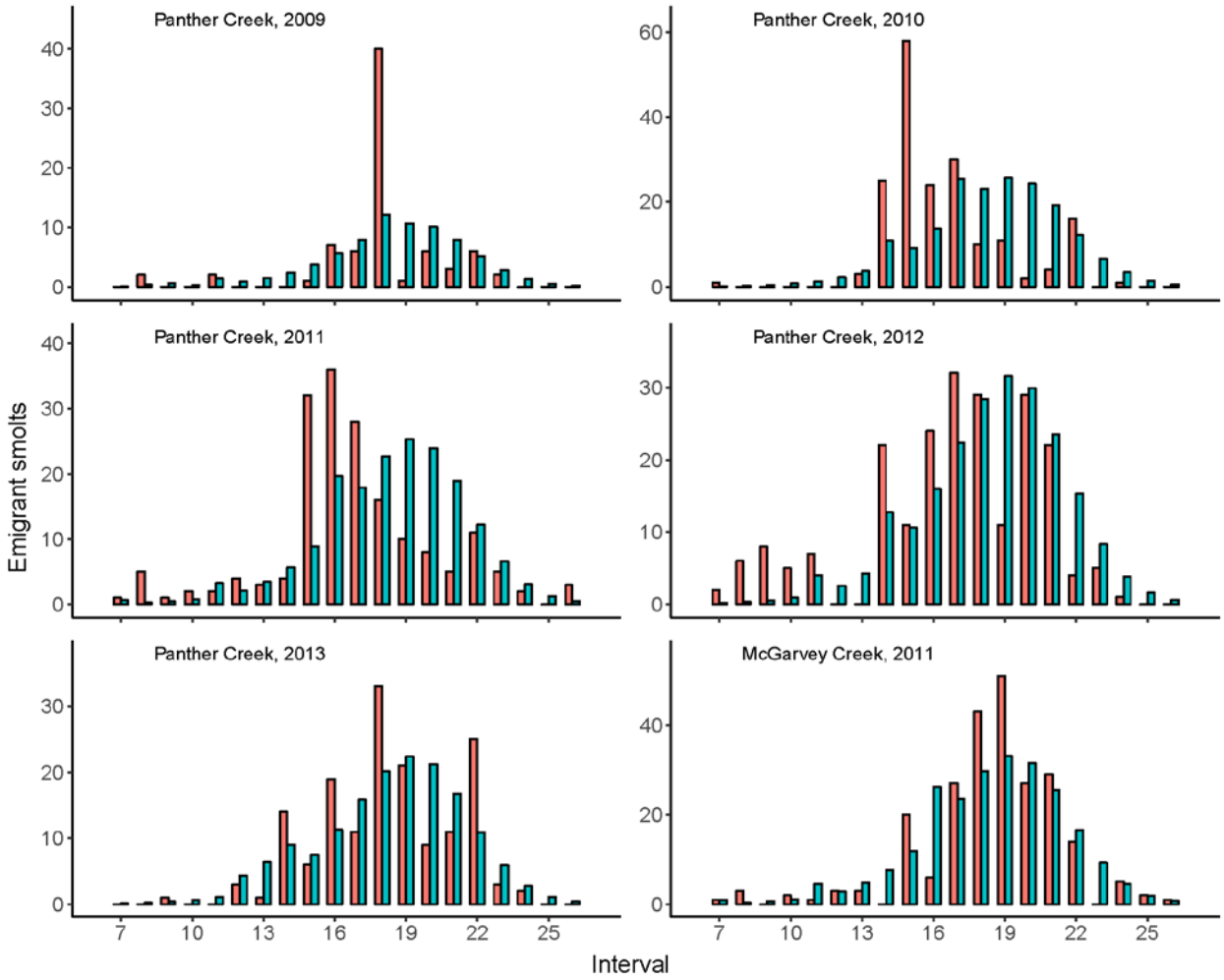

Figure 18. Frequencies of PIT-tagged smolts emigrating from Panther Creek and McGarvey Creek during seven-day intervals as predicted by the model of smolt emigration timing (blue) and as detected by stationary PIT arrays (red). Note that y-axis scales vary among years.

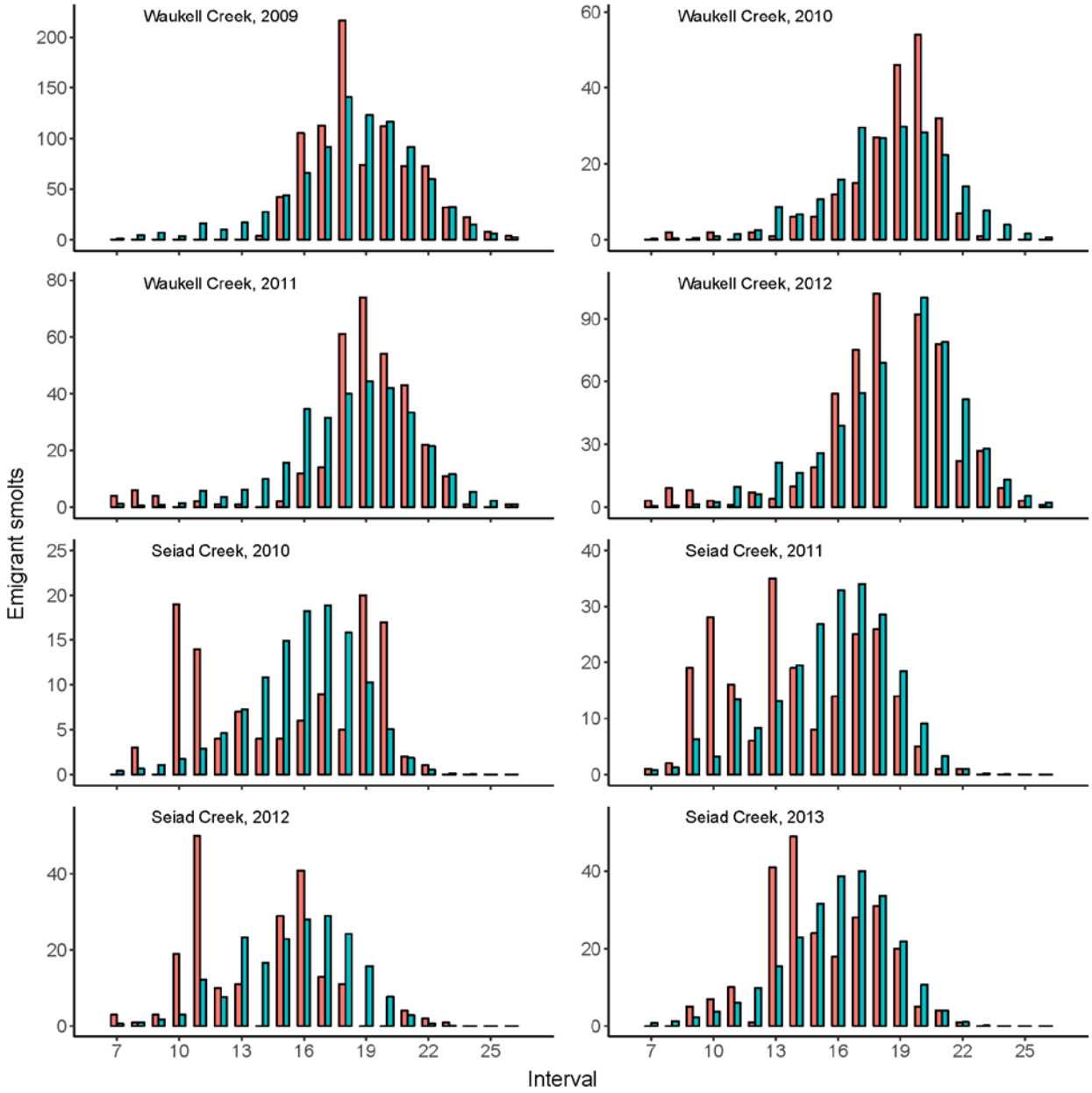

Figure 19. Frequencies of PIT-tagged smolts emigrating from Waukell Creek and Seiad Creek during seven-day intervals as predicted by the model of smolt emigration timing (blue) and as detected by stationary PIT arrays (red). Note that y-axis scales vary among years.

Mainstem migration rates ·

We assembled datasets of estimated mainstem migration rates during the summer and winter redistribution periods based on individual PIT tagged parr that were observed at different locations in the Klamath Basin during their capture histories. We fit the datasets, which consisted of 41 paired observations in summer and 161 paired observations in winter, to separate log-normal distributions. The estimated parameters of the log-normal distribution (Table 34) for the summer dataset were μ = 1.507 and σ = 1.194. This estimate of μ translated to a mean migration rate of 4.513 km per day on the arithmetic scale. The estimated parameters of the log-normal distribution for the winter dataset were μ = 1.866 and σ = 1.088, which translated to a mean migration rate of 6.462 km per day on the arithmetic scale. Density curves, constructed by drawing 1,000 random samples from a log-normal distribution with μ and σ set equal to the corresponding estimates, approximated the distributions of migration rates during the summer and winter redistribution periods (Figures 20, 21).

The advection-diffusion model (Table 34) estimated that α_r was 3.009 and β_r was 2.667, which indicated that the mean mainstem migration rate in the summer was 3.009 km/d and the mean migration rate in the winter was 5.676 km/d. The model estimated that α_σ was 20.126 and β_σ was 8.038, which indicated that the rate of spreading in the summer was 20.126 km/d$^{1/2}$ and the rate of spreading in the winter was 28.164 km/d$^{1/2}$.

Table 34. Summary of parameter estimates from two different analytical methods that were used to estimate mainstem migration rates of redistributing parr. The parameters of the log-normal distribution, μ and σ, were separately estimated for parr redistributing in summer and in winter. The parameters for the advection-diffusion model include an intercept (α) and slope (β) corresponding to the difference in advection (r) and diffusion (σ) rates between parr redistributing in summer and in winter.

Method	Parameter	Estimate
Log-normal distribution	μ_s	1.507
	σ_s	1.194
	μ_w	1.866
	σ_w	1.088
Advection-diffusion model	α_r	3.009
	β_r	2.677
	α_σ	20.126
	β_σ	8.038

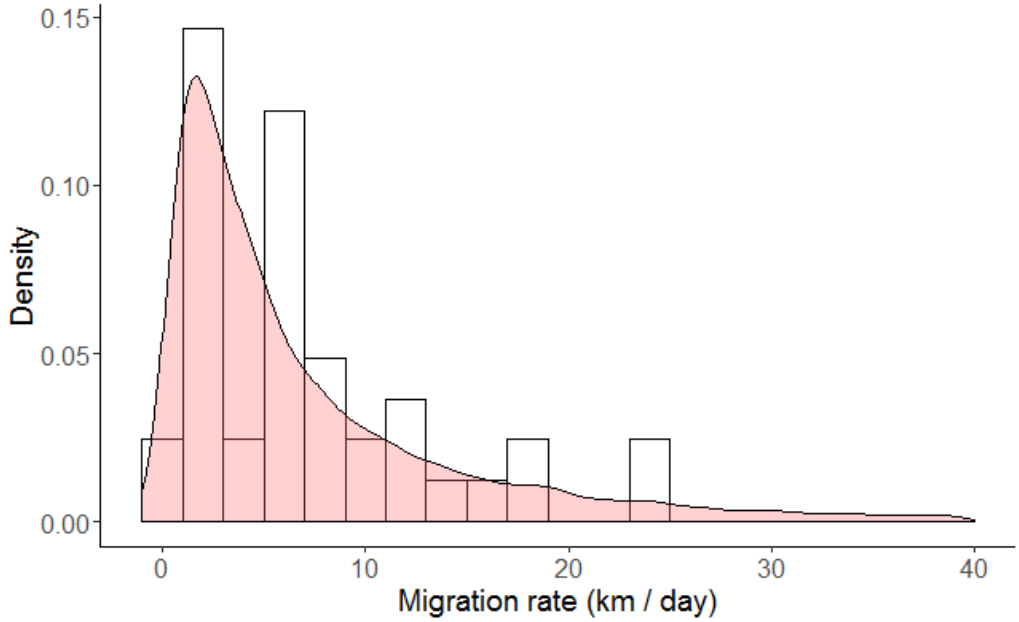

Figure 20. Histogram of migration rates in the mainstem Klamath River during summer redistributions. Migration rates were computed from 41 paired observations of age-0+ Coho Salmon. A log-normal distribution with parameters estimated from the dataset is depicted by a density curve.

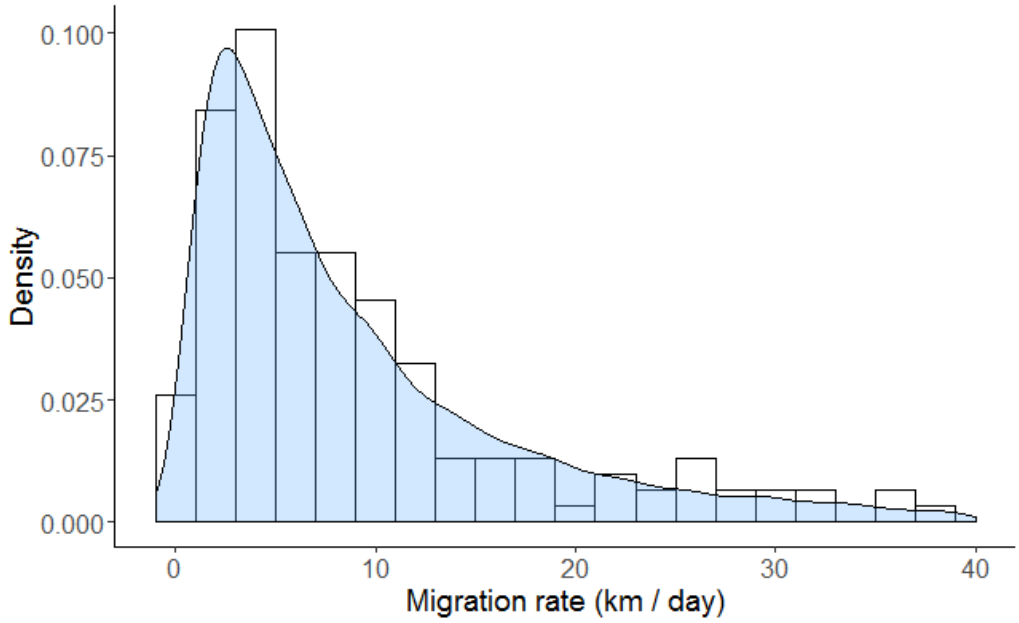

Figure 21. Histogram of migration rates in the mainstem Klamath River during winter redistributions. Migration rates were computed from 161 paired observations of juvenile Coho Salmon. A log-normal distribution with parameters estimated from the dataset is depicted by a density curve.

Discussion

The Ricker models of juvenile abundance produced several differences between tributaries to the Klamath River and life stages that warrant consideration. In the Scott River, the fit of the parr abundance model indicated that the production of this life stage may be density dependent. However, it should be noted that this relationship appeared to arise from only two data points (Figure 6) and may therefore be spurious. The Ricker models of parr abundance in the Shasta River and of smolt abundance provided little evidence of density dependence in either river, indicating that the carrying capacity of these systems was not reached during recent years (Figure 6, 7). It is not surprising to observe linearity in the spawner-recruit dynamics of these rivers given that spawning runs over the past decade have averaged 850 adults in the Scott River and 120 adults in the Shasta River, population sizes that are likely too low to induce compensatory mortality. In the Shasta River, we observed little evidence of substantial effects of environmental covariates that we considered on the productivity of either life stage. In the Scott River, by contrast, the best-fit models of productivity of each life stage included environmental covariates. The addition of environmental covariates to the Scott River models resulted in a dramatic improvement over models with spawner abundance alone. For instance, the estimated R2 of the parr abundance model improved from 0.26 to 0.88 with the inclusion of discharge during the adult migration and discharge during the spring rearing stage, and the estimated R2 of the smolt abundance model improved from 0.48 to 0.96 with the inclusion of temperature during the summer and discharge during the winter. The strong contrast in the prominence of environmental drivers in these two rivers may be a result of substantial differences in the magnitude of variation in stream conditions. Three of the four covariates that were supported in the Scott River models were indices of discharge, and the Scott River exhibits much stronger seasonal and interannual variation in discharge than the Shasta River (Figures 3, 4).

The multistate mark-recapture models produced very precise estimates of overwinter survival rates and winter emigration rates among the three surveyed locations. Excluding 2012 at Seiad Creek, in which monitoring was marred by low detection probabilities and extended antenna outages, the standard errors of the survival and emigration rates were all 0.07 or lower. These high levels of precision are the product of large releases of PIT-tagged fish and high detection probabilities, and demonstrate that our estimates of these important demographic rates are highly informed. There was a substantial amount of variability in annual survival rates, which ranged between 0.23 and 0.57 among years. However, because the annual rate is influenced by average time between tagging and detection, which fluctuates in accordance with sampling methods, the monthly survival rate is a more informative metric for population modeling. The range of the monthly rate was 0.78 - 0.91, which amounts to a substantial cumulative survival difference over the length of the overwintering period. For instance, over a six-month period, the corresponding range of cumulative survival rates is 0.22 - 0.57. While there was considerable interannual variation in the monthly survival rate at each site, there was little evidence to suggest that any one site produced particularly high survival rates. In fact, the mean monthly survival rates were remarkably similar among sites (Waukell = 0.845, McGarvey = 0.848, Seiad = 0.857). This observation supports the extension of survival rates estimated here to other streams in the

Klamath Basin. There was considerably less variation in winter emigration rates; excluding 2010 at McGarvey Creek, where we estimated an emigration rate of 0.44, the winter emigration rate ranged between 0.19 and 0.24. These differences are small enough to suggest that emigration rates estimated here may be successfully extended to some streams and years not included in our model dataset. However, streams may exhibit dramatically different migration patterns, even when they are proximate. For instance, migrant trapping conducted in the lower Klamath Basin suggested that, while Waukell Creek and McGarvey Creek both function as destinations for winter migrants from other streams, only McGarvey Creek exports large numbers of its own fish (Soto et al. 2016). These discrepancies may reflect differences in the quality of overwintering habitat at these sites.

We estimated separate adult migration timing models for the Scott and Shasta Rivers under the assumption that distinct water use patterns in those rivers would give rise to distinct migratory behaviors. We also estimated an adult migration timing model for Bogus Creek, a stream with naturally regulated flows, under the assumption that migratory behaviors observed in that stream would be a reasonable proxy for most other tributaries in the Klamath Basin. A ubiquitous feature of the three models was support for a positive effect of weekly mean temperature, which exhibited a negative interaction with photoperiod. This effect and interaction indicate that there is a tendency of adults to enter tributaries during periods of elevated water temperature, and that this tendency is more pronounced later in the migration period. However, the biological interpretation of this pattern is not straightforward. While warmer waters may be beneficial to developing embryos, the adult migration occurs during a cooling period and temperature would therefore seem to be a poor migratory cue. The primary feature that distinguished the Scott and Shasta River models from the Bogus Creek model was an increased responsiveness of migratory behavior to discharge in the former. The Scott and Shasta River models each supported a positive effect of an index of discharge. Discharge in these rivers can remain low even into early winter (Figures 3, 4), and these migratory patterns suggest that maintenance of adequate discharge may be critical to enabling timely spawning migrations. In streams with naturally regulated flows like Bogus Creek, winter precipitation patterns may provide consistently adequate discharge during the spawning migration.

The summer and winter redistribution models produced results that were consistent with expectations. That is, the transition from the mainstem to refugia was primarily driven by temperature during the summer and discharge during the winter. These patterns suggest that juveniles moving in and out of the mainstem are actively seeking habitats that provide more favorable rearing conditions, which is consistent with the life history of Coho Salmon in Northern California (reviewed by Lestelle 2007). These redistributions nearly exclusively involve downstream movement in the mainstem, and fish that redistribute may significantly shorten the length and duration of their seaward migration (Tables 14, 15). Because warming of the mainstem Klamath River in spring and summer increases the virulence of the myxozoan parasite *Ceratonova shasta*, a significant pathogen and source of mortality for juvenile Coho Salmon (Ray et al. 2012), a reduction in the length and duration of the seaward migration may confer heightened survival in smolts. Recent losses of juvenile Coho Salmon in the Klamath River from *C. shasta* infection are atypical (Margolis et al. 1992) and indicate that the parasite-host balance has been disrupted by changes in water flow and temperature associated with anthropogenic activities. Given the increasing challenges posed to migrating smolts by these environmental stressors, the behavior of redistributing during

winter when pathogen loads in the mainstem are minimal could be undergoing positive selection. The magnitude of the fitness gain conferred by redistributing is dependent on the amount of additional overwinter mortality that results from undertaking long mainstem migrations during winter. Unfortunately, little is known about mainstem mortality rates of age-0+ Coho Salmon in the Klamath River and there remains a need for studies that are specifically tailored to address this life history component.

A reoccurring observation from the smolt migration timing models was the importance of changes in discharge as a migratory trigger. In tributaries with naturally regulated flows, our smolt migration model indicated that there is an increased likelihood of emigrating during periods of increasing discharge, an observation that is consistent with previous research on migratory patterns of Coho Salmon smolts (Spence and Dick 2014). Conversely, in the artificially regulated Scott and Shasta Rivers, our smolt migration models indicated that emigration probability increases dramatically during and following periods of decreasing discharge and that this response is heightened early in the emigration period. This behavior may be a local response that enables smolts to leave these rivers before they undergo seasonal declines in water quality associated with irrigation or may be a response to rapidly declining habitat area as the flows recede. Importantly, our results suggest the potential for water management alternatives to impact the migratory behavior of Coho Salmon residing in the Klamath Basin.

This report has documented the methods and results for a large number of Coho Salmon-specific analyses directly related to demographics processes in the Klamath Basin. The analyses described in this report demonstrate that environmental variation, temperature and flow in particular, drives many components of the freshwater rearing phase of Klamath River Coho Salmon, including freshwater productivity and migration events. The sub models developed from these analyses will require basin-wide temperature and flow data, which have been compiled from extensive monitoring in the Klamath Basin and estimated from predictive models in instances when data were missing (Jones et al. 2016; Manhard et al. 2017). These sub models will eventually be linked as part of a freshwater dynamics model which will produce juveniles in naturally and artificially regulated tributaries, move them between tributaries during redistribution events, move them into the mainstem Klamath River during the smolt emigration, and move them through the mainstem and into the ocean. There remains a need to develop a mainstem migration sub model that moves smolts to the ocean. Fortunately, this aspect of Coho Salmon life history is well studied in the Klamath River. A radio telemetry study tracked four brood years of Coho Salmon smolts in the mainstem Klamath River and evaluated how environmental variation influenced their migration and survival rates (Beeman et al. 2012). The results of that study will be used to develop a mainstem migration sub model for smolts, which will be linked with the sub models described in this report to form a complete freshwater dynamics model.

Literature Cited

Bates D., M. Maechler, B. Bolker, and S. Walker. 2015. Fitting Linear Mixed-Effects Models Using lme4. Journal of Statistical Software 67(1): 1-48.

Beeman J., S. Juhnke, G. Stutzer, and K. Wright. 2012. Effects of Iron Gate Dam Discharge and Other Factors on the Survival and Migration of Juvenile Coho Salmon in the Lower Klamath River, Northern California, 2006–09. U.S. Geological Survey Open-File Report 2012-1067, 96 p.

Beschta R. L., and R. L. Taylor. 1988. Stream temperature increases and land use in a forested Oregon watershed. Water Resources Bulletin 24: 19-25.

Brett J. R. 1952. Temperature tolerance in young Pacific salmon, genus Oncorhynchus sp. Journal of the Fisheries Research Board of Canada 9: 265-323.

Burnham K. P., and D. R. Anderson. 2002. Model selection and multimodel inference: a practical information theoretic approach. Springer, New York, N.Y.

Carlson S. R., L. G. Coggins Jr, and C. O. Swanton. 1998. A simple stratified design for mark-recapture estimation of salmon smolt abundance. Alaska Fishery Research Bulletin 5(2): 88-102.

Chesney D., and M. Knetchle. 2016. 2015 Shasta River chinook and coho salmon observations in Siskiyou County, CA. California Department of Fish and Game.

Gelman A., and D. B. Rubin. 1992. Inference from iterative simulation using multiple sequences. Statistical Science 7: 457-472.

Hijams R. J. 2016. geosphere: Spherical Trigonometry. R package version 1.5-5. https://CRAN.R-project.org/package=geosphere

Jones E. C., R. W. Perry, J. C. Risley, N. A. Som, and N. J. Hetrick. 2016. Construction, calibration, and validation of the RBM10 water temperature model for the Trinity River, Northern California. U.S. Geological Survey Open-File Report 2016-1056, 46 p.

Knecthle M., and D. Chesney. 2016. 2015 Scott River salmon studies, final report. California Department of Fish and Game.

Lestelle L. 2007. Coho salmon (Oncorhynchus kisutch) life history patterns in the Pacific Northwest and California. Biostream Environmental.

Manhard C. V., N. A. Som, E. C. Jones, and R. W. Perry. 2017. Estimation of stream conditions in tributaries of the Klamath River, Northern California. U.S. Geological Survey Open-File Report 2016-XX , 27 p.

Margolis L., T. E. McDonald, and D. J. Whitaker. 1992. Assessment of the impact of the myxosporean parasite Ceratomyxa shasta on survival of seaward migrating juvenile Chinook salmon, Oncorhynchus tshawytscha, from the Fraser River, British Columbia. Canadian Journal of Fisheries and Aquatic Sciences. 49:1883-1889

McCullagh P., and J. A. Nelder. 1989. Generalized linear models. 2nd ed. Chapman and Hall, London.

Mohseni O., H. G. Stefan, and T. R. Erickson. 1998. A nonlinear regression model for weekly stream temperatures. Water Resources Research 34(10): 2685-2692.

Plummer M. 2003. JAGS: A program for analysis of Bayesian graphical models using Gibbs sampling.

Plummer M. 2016. rjags: Bayesian Graphical Models using MCMC. R package version 4-6. https://CRAN.R-project.org/package=rjags

Poisot T. 2011. The digitize package: extracting numerical data from scatterplots. The R Journal 3(1): 25-26.

R Core Team. 2016. R: A language and environment for statistical computing. R Foundation for Statistical Computing, Vienna, Austria.

Ray R. A., R. A. Holt, and J. L. Bartholomew. 2012. Relationship between temperature and C. shasta-induced mortality in Klamath River salmonids. Journal of Parasitology 98(3) 520-526.

Soto T., D. Hillemeier, S. Silloway, A. Corum, A. Antonetti, M. Kleeman, and L. Lestelle. 2016. The role of the Klamath River mainstem corridor in the life history and performance of juvenile coho salmon (Oncorhynchus kisutch). U.S. Bureau of Reclamation Submission.

Spence B. C., and E. J. Dick. 2014. Geographic variation in environmental factors regulating outmigration timing of coho salmon (Oncorhynchus kisutch) smolts. Canadian Journal of Fisheries and Aquatic Sciences 71: 56-69.

Stocking R. W., and J. L. Bartholomew. 2007. Distribution and habitat characteristics of Manayunkia speciosa and infection prevalence with the parasite Ceratomyxa shasta in the Klamath River, Oregon-California. Journal of Parasitology 93(l): 78-88.

Venables W. N. and B. D. Ripley. 2002. Modern Applied Statistics with S. Fourth Edition. Spring, New York.

Weitkamp L. A. , T. C. Wainwright, G. J. Bryant, G. B. Milner, D. J. Teel, R. G. Kope, and R. S. Waples. 1995. Status Review of Coho Salmon from Washington, Oregon, and California. NOAA Technical Memorandum NMFS-NWFSC-24. 258 p.

Zabel R. W. and J. J. Anderson. 1997. A model of travel time of migrating juvenile salmon with an application to Snake River spring Chinook salmon. North American Journal of Fisheries Management 17: 93-100.